RAÍSA BRITO VILELA

EVALUATION OF AIRBORNE GAMMA-RAY SPECTROMETRY IN CONTRASTING LANDSCAPES UNDER TROPICAL CONDITIONS

LAVRAS – MG

2021

RAÍSA BRITO VILELA

EVALUATION OF AIRBORNE GAMMA-RAY SPECTROMETRY IN CONTRASTING LANDSCAPES UNDER TROPICAL CONDITIONS

Dissertação apresentada à Universidade Federal de Lavras, como parte das exigências do Programa de Pós-Graduação em Ciência do Solo, área de concentração em Recursos Ambientais e Uso da Terra, para a obtenção do título de Mestre.

Profa. Dra. Michele Duarte de Menezes

Orientadora

LAVRAS - MG

2021

Ficha catalográfica elaborada pelo Sistema de Geração de Ficha Catalográfica da Biblioteca Universitária da UFLA, com dados informados pelo(a) próprio(a) autor(a).

Vilela, Raísa Brito.
Evaluation of airborne gamma-ray spectrometry in contrasting landscapes under tropical conditions / Raísa Brito Vilela. - 2021.
62 p. : il.

Orientador(a): Michele Duarte de Menezes.

Dissertação (mestrado acadêmico) - Universidade Federal de Lavras, 2021.
Bibliografia.

1. Airborne gamma-ray spectroscopy. 2. Contrasting landscapes. 3. Tropical environment. I. de Menezes, Michele Duarte. II. Título.

RAÍSA BRITO VILELA

EVALUATION OF AIRBORNE GAMMA-RAY SPECTROMETRY IN CONTRASTING LANDSCAPES UNDER TROPICAL CONDITIONS

AEROGAMAESPECTROMETRIA EM AMBIENTES CONTRASTANTES SOB CONDIÇÕES TROPICAIS

Dissertação apresentada à Universidade Federal de Lavras, como parte das exigências do Programa de Pós-Graduação em Ciência do Solo, área de concentração em Recursos Ambientais e Uso da Terra, para a obtenção do título de Mestre.

APROVADA em 30 de julho de 2021.

Dra. Michele Duarte de Menezes - UFLA

Dr. Bruno Teixeira Ribeiro - UFLA

Dr. Élvio Giasson - UFRGS

Prof. Dra. Michele Duarte de Menezes

Orientadora

LAVRAS – MG

2021

AGRADECIMENTOS

À FAPEMIG, o presente trabalho foi realizado com apoio da Fundação de Amparo à Pesquisa de Minas Gerais (FAPEMIG).

À Capes e CNPq pelos incentivos a pesquisa científica.

Ao DCS/UFLA, pela oportunidade e ensinamentos.

À Companhia de Desenvolvimento de Minas Gerais (CODEMGE) por gentilmente ceder informações dos levantamentos aerogeofísicos (ofício n.153/2019/GAB/UFLA).

À Professora Michele, pelo conhecimento passado, orientação, compreensão e paciência.

Aos colegas Maria Eduarda, pela amizade e generosidade, e Marcelo, pelo apoio.

Agradeço aos Céus pela vida, saúde e proteção minha e dos que me cercam.

À minha mãe Cláudia e ao meu pai Márcio e toda minha família, pelo suporte e amor incondicional.

Ao Vinícius, por toda ajuda, incentivo e carinho.

Agradeço a todos que contribuíram e me ajudaram de alguma forma nessa caminhada.

GENERAL ABSTRACT

The area of this work is located in the south region of Minas Gerais State, which presents a great geological complexity, along with different geomorphological landscapes and soil types, with predominance of the weathered soils. The study area has a reliable and high resolution airborne gamma-ray spectrometry survey throughout its territory performed by the former Economic Development Company of Minas Gerais (CODEMIG) in partnership with CPRM (Brazil Geological Service). Airborne gamma-ray spectroscopy detects the natural gamma radiation in the upper 30 cm of the Earth's surface. The gamma-ray emitting isotopes used in this passive remote sensing are ^{40}K, ^{238}U and ^{232}Th decay series. These are used to infer K, U and Th concentrations. The integrated use of gamma spectrometric images with digital elevation models has great potential for application in soil sciences and has been widely used for regolith mapping, landscape evolution research, environmental applications and others. In Brazil, the usage applies predominantly to geological mapping and mineral exploration. This master's dissertation aims to open paths for the use of these data in the department of soil science and also to understand the aspects that involve the use of these data in the tropical environment. For this purpose, the dissertation is divided in two parts. The first one presents theorical reference about principles of gamma-ray spectrometry and a compilation of scientific papers published regarding soil science. The second part has a scientific article which aims: I) understand the influence of environmental attributes on the dynamics of %K, eTh and eU contents obtained by airborne sensing in contrasting landscapes of south Minas Gerais; II) understand how pedogenesis changes the radioelements signature in tropical landscapes; III) evaluate the potential of gamma spectrometric images in mapping soil's parent material for regional studies. To achieve these goals gamma spectrometric responses were compared in landscapes at different geomorphological stages for four distinct lithological groups.

Keywords: Airborne gamma-ray spectrometry. Contrasting landscapes. Lithological groups

RESUMO

A área deste trabalho está localizada na região sul do Estado de Minas Gerais, que apresenta uma grande complexidade geológica, juntamente com diferentes paisagens geomorfológicas e tipos de solo, com predominância dos solos intemperizados. A área de estudo conta com levantamento aerogamaespectrométrico confiável e de alta resolução em todo o seu território, realizado pela antiga Companhia de Desenvolvimento Econômico de Minas Gerais (CODEMIG) em parceria com a CPRM (Serviço Geológico do Brasil). A aerogamaespectrometria detecta a radiação gama natural nos 30 cm superiores da superfície da Terra. Os isótopos emissores de raios gama usados neste sensoriamento remoto passivo são as séries de decaimento do ^{40}K, ^{238}U e ^{232}Th. Eles são usados para inferir as concentrações de K, U e Th. O uso integrado de imagens gamaespectrométricas com modelos de elevação digital tem grande potencial em ciências do solo e tem sido amplamente utilizado para mapeamento de regolito, pesquisa de evolução de paisagem, aplicações ambientais e outros. No Brasil, o uso se aplica predominantemente ao mapeamento geológico e à exploração mineral. Esta dissertação de mestrado visa abrir caminhos para a utilização desses dados no departamento de ciências do solo e também compreender os aspectos que envolvem o uso desses dados no ambiente tropical. Para tanto, a dissertação está dividida em duas partes. A primeira apresenta um referencial teórico sobre os princípios da aerogamaespectrometria e uma compilação de artigos científicos publicados a respeito da aplicação na ciência do solo. A segunda parte contém um artigo científico que visa: I) compreender a influência dos atributos ambientais na dinâmica das concentrações de %K, eTh e eU obtidos por Aerogamaespectrometria em paisagens contrastantes do sul de Minas Gerais; II) compreender como a pedogênese altera a assinatura de radioelementos em paisagens tropicais; III) avaliar o potencial das imagens gamaespectrométricas no mapeamento do material de origem do solo para estudos regionais. Para atingir esses objetivos, as respostas gamaespectrométricas foram comparadas entre paisagens em diferentes estágios geomorfológicos para quatro grupos litológicos distintos.

Palavras-chave: Aerogamaespectrometria. Paisagens contrastantes. Grupos litológicos

SUMMARY

FIRST PART

1 INTRODUCTION

Airborne geophysical surveys have been carried out in Brazil since 1952 sponsored by federal institutions. In 2001, a new phase in geophysical aerial surveys has begun, where most of gamma-ray spectrometry projects were acquired with higher resolution (flight height of 100 m). In Minas Gerais, aerogeophysical survey programs lead by Companhia de Desenvolvimento de Minas Gerais (Codemig), Serviço Geológico do Brasil (CPRM), and Agência Nacional de Petróleo, Gás Natural e Biocombustíveis (ANP) covered the entire state (CODEMGE, 2019).

Gamma-ray spectrometry consists of measuring the concentration of radioisotopes K, eTh and eU in rocks and weathered materials by detecting and quantifying the gamma radiation emitted by the natural radioactive decay of these elements (MINTY, 1997). The acquisition of such information was mainly devoted to assisting mineral and geological exploration due to the potential for locating mineral exploration targets. Besides geological exploration, other studies have shown potential application of this information for environmental diagnosis of contaminated areas (SANTOS, MENESES, NASCIMENTO, 2009), mapping regolith and land management strategies (WILFORD; BIERWIRTH; CRAIG, 1997), development of weathering index (WILFORD, 2012), mapping soil properties (ROUZE; MORGAN; McBRATNEY, 2017), and others. In Brazil, Mello et al. (2021) confirms the great potential of gamma-ray spectrometry using proximal sensor. However, products from remote sensing have as advantage the extensive and fast spatial data cover. Besides their great potential, further studies are still necessary under tropical conditions in order to better understand the gamma-ray contents in different soil parent material, where weathering and leaching conditions could be the most intense in the world.

Thus, this dissertation is divided into two parts. The first one presents the theoretical framework about principles of gamma-ray spectrometry and a compilation of scientific papers published regarding soil science. In addition, a geological and pedological characterization of the south region of Minas Gerais was carried out. The second part consists of a scientific article containing a study case carried out to explore the relationship among %K, eTh and eU with contrasting conditions of soil, geology, relief, and climate in the south of Minas Gerais state. Representative areas containing rock outcrops and Red Latosols were selected, since they represent the most contrasting conditions of weathering stage. The specific objectives were: i)

to understand the influence of environmental attributes on the dynamics of the radionucleotides; ii) to understand how pedogenesis changes the radioelements signature in tropical landscapes; iii) to evaluate the potential of gamma spectrometric images in mapping soil parent material for regional studies.

2 THEORETICAL REFERENCES

2.1 Principles of gamma-ray spectrometry

The geophysical survey involves taking measurements on or near Earth's surface. The measurements are influenced by the internal distribution of the physical properties of the Earth, whose analyzes can show how the physical properties of the Earth's interior vary vertically and laterally. Geophysical surveys, although subject to interpretation ambiguities or uncertainties, have provided a relatively quick and cheap way to obtain distributed information of Earth's subsurface (KEAREY; BROOKS; HILL, 2002). An example of geophysical method is the aerial gamma-ray spectrometry, a passive remote-sensing technique. It involves measurements of natural gamma radiation of surface materials. The gamma rays are photons of energy emitted from the decay of radioactive isotopes. Each photon has a discrete energy, which is characteristic of an isotope allowing for the diagnosis of the radiation source. Energies of geological interest range from 0.2 to 3 MeV, corresponding to eletromagnetic wavelengths of approximately 3×10^{-12} m and about 3×10^{19} Hz of frequency. Regarding the aerial surveys, it detects the natural gamma radiation in the upper 30 cm of the Earth's surface.

There are three sources of natural gamma radiation: (1) ^{40}K, ^{238}U, ^{235}U, and ^{232}Th related to the origin of the solar system; (2) radioactive daughter products of the first ones; (3) isotopes created by external causes such as the interaction between cosmic rays and Earth atmosphere (KOGAN; NAZAROV; FRIDMAN, 1969; MINTY, 1997). However, the only natural radioactive elements capable of releasing intense and energetic gamma radiation that can be measured by airborne survey are Uranium, Thorium and Potassium (MINTY, 1997).

The average crustal concentration of U is 2.7 ppm and the element occurs as the natural radioactive isotopes ^{238}U and ^{235}U, which decay series end in the stable isotopes ^{206}Pb and ^{207}Pb, respectively. ^{235}U represents only 0,72% of natural U, and its gamma-ray energy decay is not captured by airborne gamma-ray surveying. Th occurs as radioisotope ^{232}Th, and decay through a series of daughter nuclides until the stable ^{208}Pb. K average crustal abundance is 2% and it has only one radioactive isotope, which is the ^{40}K that represents 0,012% of natural K. There is

a 11% probability of ^{40}K decay to ^{40}Ar, this is followed by emission of a gamma-ray photon of 1,46 MeV (MINTY, 1997).

Since 40K constitutes 0,02% of natural K, the gamma-ray surveyed by measurement of the 1,46 MeV gamma-ray emitted by decay of 40K to 40Ar is, therefore, a direct measurement of K content in rocks and weathered materials (DICKSON; SCOTT, 1997; MINTY, 1997; WILFORD; BIERWIRTH; CRAIG, 1997). The abundance of U and Th are measured counting distinct emission peaks of their daughter nuclides ^{214}Bi and ^{208}Tl, respectively. This methodology assumes secular equilibrium in the ^{238}U and ^{232}Th decay series. For this reason, U and Th are expressed as equivalent part per million eU (Bi – 1,76MeV) and eTh (Tl – 2,61Mev) indicating that their concentrations are inferred from daughter elements. Because of elevated crustal concentration, K is expressed in percentage (%K) (COOK et al., 1996; DICKSON; SCOTT, 1997; MINTY, 1997; WILFORD; BIERWIRTH; CRAIG, 1997).

Disequilibrium in the decay chain can occur by removal or concentration of one or more daughter products. In such cases, the measured isotopes Bi and Tl in the U and Th decay series, respectively, may not quantify with accuracy the parent isotopes. Therefore, gamma-ray data interpretation must consider disequilibrium, especially when correlating aerial gamma ray spectrometry data with rock or soil samples (MINTY, 1997; WILFORD; BIERWIRTH; CRAIG, 1997).

Intensity of gamma radiation emitted from the surface depends on mineralogy and geochemistry of rocks, soils and the nature of weathering (WILFORD; BIERWIRTH; CRAIG, 1997). K occurs predominantly in alkali primary minerals such potassic feldspars (e.g. orthoclase and microcline) and micas (e.g. biotite and muscovite), and it is absent on mafic minerals. Hence, K has relatively high concentration on felsic rocks (e.g. granites, rhyolites, and others), but low on mafic rocks (e.g. basalts), and very low on ultramafic rocks (e.g. dunites and peridotites). During the weathering of K-bearing primary minerals biotite, K-feldspar, and muscovite will be destroyed. The K released is adsorbed in the formation of K-bearing clay minerals as illite, montmorillonite, and in less amounting kaolinite. K is a mobile and soluble element on weathering conditions, and the adsorption of K by clays is reflected in the low concentrations of K in sea water (DICKSON; SCOTT, 1997; WILFORD; BIERWIRTH; CRAIG, 1997).

U is a relative rare element on crustal composition (~3 ppm) and it is found in two valence states U^{4+} and U^{6+}. U^{4+} is usually found in insoluble minerals. The oxidized form U6+ generally complexes with anions as CO_3^{2-}, SO_4^{2-}, and PO_4^{3-} forming soluble minerals (LANGMUIR, 1978; WILFORD; BIERWIRTH; CRAIG, 1997). U^{6+} mobility is changed by

adsorption to hydrous iron oxides, clay minerals and colloids and by reduction to insoluble U^{4+} minerals on reducing environments. U occurs: in rocks as oxide and silicate minerals of uraninite and uranothorite, mainly in monazite, xenotime and zircon; as trace elements in other rock-forming minerals; along grain boundaries as oxides or silicates (DICKSON; SCOTT, 1997). Zircon and monazite are the only U-bearing minerals that remain stable during weathering. The U released by U-bearing minerals weathering may be retained in authigenic iron oxides and clay minerals, or precipitated under reducing conditions (DICKSON; SCOTT, 1997).

Th is also a minor element on the Earth's crust (~12ppm). It occurs in valence state Th+4 (DICKSON; SCOTT, 1997), and has low solubility, except in acid solutions (LANGMUIR; HERMAN, 1980). Organic compounds such as humic acids may increase Th solubility in neutral pH conditions (CHOPPIN, 1988). According to Dickson and Scot (1997), Th may be present in allanite, monazite, xenotime, and zircon at levels higher than 1000 ppm or as trace element in other rock forming minerals. Monazite and zircon are the major Th-bearing minerals, and due to their stability, they may accumulate in heavy mineral sand deposits. Th released by weathering may be retained onto Fe or Ti oxides or hydroxides, and clays. As U, Th may be absorbed onto iron oxides and colloidal clays (DICKSON; SCOTT, 1997).

The distribution of the radioelements K, U, and Th in Australian rocks and soils were studied by Dickson and Scott (1997) using proximal gamma-ray sensing. The data showed that for igneous rocks there is a trend for increasing radioelement content with increasing of Si content, despite differences between K, U and Th concentrations. Felsic rocks showed higher concentrations of radioelements than ultrabasic and mafic rock, in which Th showed larger increase content than U (DICKSON; SCOTT, 1997). However, the authors emphasized that for a same rock type may exist in a wide range of radioelements concentration, thus global classification of rock type is not possible using radioelement contents. Perhaps, for specific regions rock types can be identified by relative content of K, U and Th. Dickson and Scott (1997) also discussed about radioelements concentration on metamorphic and sedimentary rocks. According to the authors, metamorphism usually does not affect radioelement content on rocks and sedimentary rocks, presenting radioelement concentration reflecting the parent source.

According to Wilford, Bierwirth and Craig (1997), during chemical and physical weathering, the radioelements are released from rocks, redistributed and incorporated into the

soil and regolith. Radioelements contents on regolith can differ considerably from their source rocks due to textural and geochemical reorganization in the weathering profile.

Dickson and Scott (1997) concluded that weathering results on loss of K in all rocks types. For felsic rocks there are also loss of U and Th. Typically, losses are between 20 to 30% for K, U and Th. During initial weathering, intermediate, mafic and ultramafic rocks show less change in radioelements content, but pedogenetic process can produce soils with relatively higher concentration of U and Th, increased with basicity of the rock. Then, soils derived from different lithological units can show similar radioelement content needing additional data sets and field checking for confusing signatures and anomalous areas (DICKSON; SCOTT, 1997).

2.2 Applications of airborne gamma-ray spectrometry

Gamma spectrometry was initially proposed for mineral exploration and geological mapping, with increase in applications related to pedological and environmental studies (COOK et al., 1996; DICKSON; SCOTT, 1997; THIESSEN et al., 1999; WILFORD; BIERWIRTH; CRAIG, 1997; MOONJUN et al.,2017; YOUSEEF, 2016; METELKA et al., 2018).

Cook et al. (1996) reported four potential uses of gamma-ray spectrometry: a) detection of U and Th deposits; b) geological mapping by correlation of radionuclides content with rocks types; c) geochemical anomalies trace, since radionuclides are redistributed by weathering; d) to infer erosional process. The authors examined the use of airborne gamma-ray spectrometry to detect spatial variation of soil parent material by comparing ground and airborne measurements. The authors concluded that, despite the limitations, the data provided valuable insights about the spatial distribution of soil parent materials over a large area.

According to Wilford, Bierwirth and Craig (1997), airborne gamma-ray survey provides information on geomorphological process in the landscape and regolith properties and, therefore, it is an important tool for mapping regolith, mineral exploration and land management strategies. Combining gamma-ray data with digital elevation models and other data sets can enhance the potential of this method. Wilford (2012) applied airborne gamma-ray spectrometry and digital terrain analysis to develop a weathering intensity index for the whole Australian continent. Weathering intensity index has application in understanding weathering and geomorphological processes.

Santos, Meneses and Nascimento (2009) and Souza and Ferreira (2005) applied gamma spectrometry to evaluate soil contamination by intensive and continuous application of

fertilizers. Taylor et al. (2002) investigated the relationships between soil properties and high-resolution radiometric data, and concluded that the method can assist the mapping of soil properties such as shallow granitic bedrock, presence or absence of gravel, and the percentage of clay in the first 10 cm of the soil.

Iza, Horbe and Silva (2016) used airborne gamma-ray spectrometry and altimetry to identify domains with higher probability of lateritic crust occurrence in Brazilian Amazon. The authors compared Boolean and fuzzy techniques to classify favorable areas and both methods showed good responses. These tools can contribute to geological mapping and to the knowledge about radioelement distribution in weathered materials.

Moonjun et al. (2017) evaluated the potential of airborne gamma-ray imagery for improving digital soil survey process, and the relation between gamma-ray data and geological materials. Gamma-ray and elevation data were clustered by fuzzy logic generating different classification layers. The results showed relatively higher accuracy of soil parent material differentiation then for soil types.

Rouze, Morgan and McBratney (2017) applied proximal gamma radiometric surveys through different landforms to evaluate the potential of aerial gamma radiometric for mapping soil properties. Proximal and aerial measurements comparisons were only purposeful when the latter were correctly geo-located. When it occurs, aerial gamma information significantly explained about half of clay and sand content variability comparing with proximal gamma measurements. Therefore, aerial gamma data has capability in characterizing soil spatial variability, but special attention should be given to the surveys data quality.

Youssef (2016) proposed to establish relationships between ground and airborne gamma-ray spectrometric data in a region of Egypt. For this purpose, the author examined in detail ground and airborne gamma-ray spectrometric data, in conjunction with geologic information (rock types). The ground measurements are condensed and focused while the airborne measurements are more smoothed and the relation between these two types of survey vary from one geological unit to another, so it cannot be applied on other areas since it depends on geology of each region.

Metelka et al. (2018) developed a new automatic method for regolith landform mapping combining airborne gamma-ray spectrometry data and other remote sensing data (ASTER, Landsat, ALOS PALSAR, Radarsat-2, and SRTM digital elevation model). Artificial neural network classifier was used to combine geophysics and remote sensing information. The results showed the potential of machine learning in regolith landform mapping, and that gamma ray

spectrometry and digital elevation model data were ranked as the most important inputs. The approach may be employed in mineral exploration and geomorphological research.

Mello et al. (2021a) applied proximal gamma-ray spectrometry to evaluate tropical landscape dynamics, pedogenesis and spatial distribution of radionuclides and soil attributes. Results showed that this tool has potential for improving pedosphere studies and digital soil mapping, since results showed: a direct relationship between the soil parent material composition (rocks or sediments) and radionuclide content; higher correlation between Th and Clay content, and K increasing with the increasing of soil cation exchange capacity and clay content.

2.3 Technical characterization of airborne gamma-ray spectrometry survey

2.3.1 Airborne gamma-ray spectrometry survey

Aerial gamma-ray data was obtained from aerogeophysical surveys coordinated by Minas Gerais Economic Development Company (CODEMIG) and Brazil Geological Survey (CPRM). From 2001 to 2013, the CODEMIG developed an extensive geophysical survey program in Minas Gerais (areas 1 to 21 presented in Figure 1) (CODEMGE, 2013). The study areas comprise part of the areas 2, 7, 14 and 15. Aerogeophysical survey of the south part of the study area (São José dos Campos - Resende Project) was coordinated by CPRM (Figure 1).

Figure 1 - Figure showing the aerogeophysical surveys in the study area and Minas Gerais State. The surveys on the area of interest are areas 2, 7, 14 and 15 conducted by CODEMIG and São José dos Campos – Resende Project conducted by CPRM.

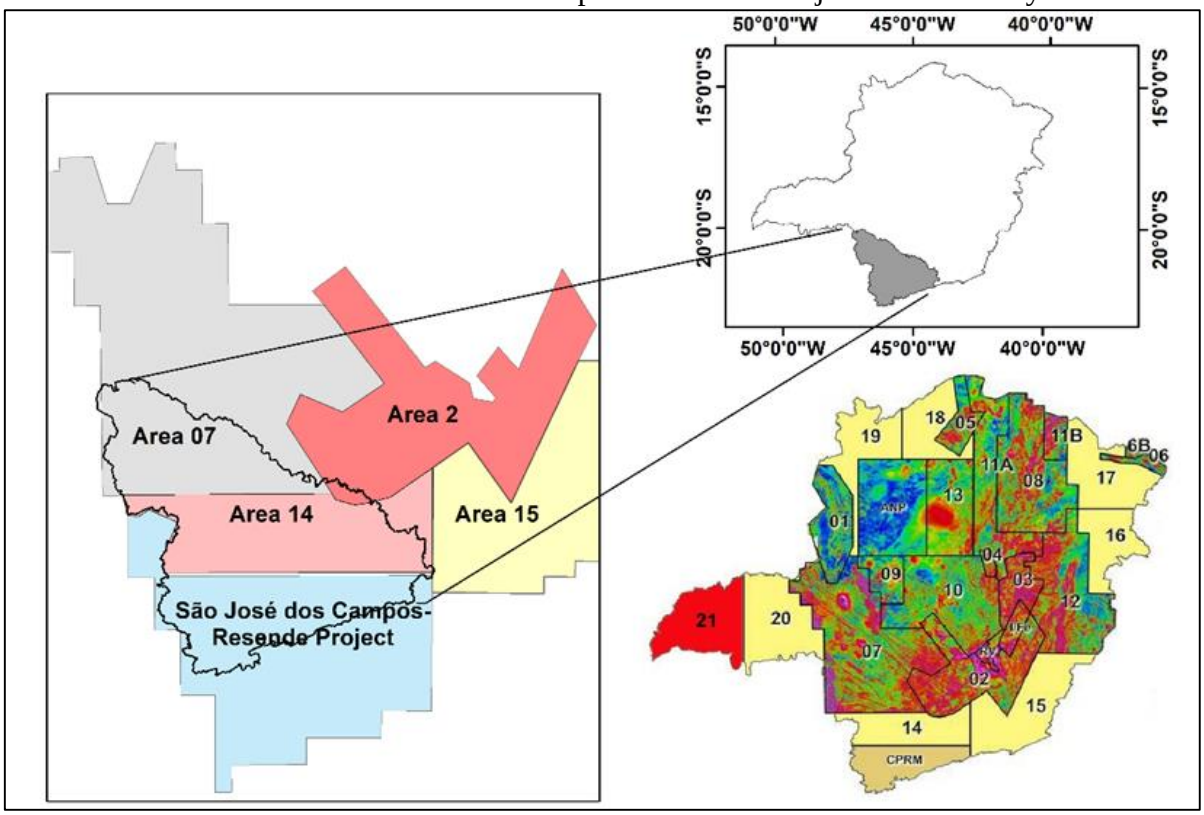

Source: Author (2021)

In area 2, prospecting and data processing were conducted by Lasa Engenharia e Prospecções S.A. in 2001. The measurements were obtained by Exploranium gamma-ray spectrometer model GR-820 coupled on a Cessna aircraft. The direction of flight profiles was N30E with a spacing of 250 m. The gamma-ray spectrometer measured at each 1,0 s corresponding about 80 m on ground (SEME, 2001).

The study area comprises the south part of area 7, where the prospection and data processing were conducted by Lasa Engenharia e Prospecções S.A. in 2006. In order to cover the area, it was performed 932 flight profiles and 45 control lines, totalizing 18,5264.98 km of geophysical profiles. The aircrafts utilized were Cessna caravan C208, Reims caravan II and Piper Navajo PA31-350 flying with an average height of 100 m and velocity of 280 km/h (CODEMIG; CPRM, 2006).

The measurements were obtained by a Exploranium gamma-ray spectrometer model GR-820. The direction of flight profiles was N-S with a spacing of 400 m, and for the control lines the direction was E-W with spacing of 800 m. The gamma-ray spectrometer measured at each 1,0 s corresponding about 78 m on ground (CODEMIG; CPRM, 2006).

The area 14 (Poços de Caldas – Varginha – Andrelândia Project) was acquired and processed by Lasa Engenharia e Prospecções S.A. in 2011. The aerogeophysical survey covered 49,353.73 km of high resolution aerial gamma-ray spectrometric profiles, with flight profiles and control lines spaced of 500 m and 1000 m, respectively, oriented in the NS and EW directions. The flight height was set at 100 m above the ground and the average velocity was of 263 Km/h (CODEMIG; CPRM, 2011).

Two aircrafts participated in the survey, Piper Navajo PA31 prefix PT-WOT and Cessna Caravan 208B prefix PT-MEP. The gamma-ray spectrometer, an Exploranium GR-820 with 256 spectral channels, measured at each 1,0 s corresponding to intervals of approximately 73 meters on terrain (CODEMIG; CPRM, 2011).

Area 15 was also conducted by Lasa Engenharia e Prospecções S.A. in 2011. The measurements were obtained by a Exploranium gamma-ray spectrometer model GR-820 coupled on a Cessna or Navajo aircraft. The direction of flight profiles was NS with a spacing of 500 m. The gamma-ray spectrometer measured at each 1,0 s corresponding about 67 m on ground (CODEMIG; CPRM, 2011).

The São José dos Campos - Resende Aerogeophysical Project, which covers the south of the study area was coordinated by CPRM and executed by Microsurvey Aerogeofísica e Consultoria Científica LTDA from 2010 to 2013. This project comprises a total area of 47,321 km2, and the geophysical covering was done by 101.085 km of high resolution aerial gamma-ray spectrometry profiles. The flight profiles direction was N-S, spaced 500 m while the control lines were E-W, spaced 10000 m (CPRM, 2013).

The aircrafts utilized were: Embraer EMB 820C Navajo, Piper PA-31-310 Navajo B, Cessna Gran Caravan. The average flights velocity and height were 265 km/h and 100 m. The gamma-ray spectrometers utilized were Exploranium GR 820, Pico Envirotec GRS410 and Radiation Solutions INC RS-500. The readings made on gamma-ray spectrometers were at each 1,0 s corresponding around 75 m of terrain (CPRM, 2013).

All the data obtained were submitted to a series of standard data processing of aerogeophysical surveys. It should be emphasized that to this study the gamma-spectrometric data were already refined and are ready for interpolation. OASIS MONTAJ software of the GEOSOFT system was used to the survey data processing (CODEMIG; CPRM, 2006, 2011; CPRM, 2013).

2.3.2 Data processing and derived products

Educational version of 9.7 OASIS MONTAJ software of Seequent company was used for data processing and interpolation. Firstly, the GDB files containing K (%), eTh (ppm) and U (ppm) data of each project were cut in relation to the study area polygon. Then, the data set were interpolated using minimum curvature in regular grids of 100 m (1/4 to 1/5 of flight line spacing) generating the grids of K, eTh and eU concentrations. Such metrics were based on technical reports commonly used for all surveys (IAEA, 2003).

The resulting grids of each area were then attached using the grid knitting tool. Visual inspection of K, eTh and eU grids showed few pixels of negative concentrations for all channels, mainly at the edges of the projects. To smooth out these negative values, the total area grids were converted on GDB (sample a grid tool) and using a mask tool the negative values of each channel were replaced by zero and again interpolated by minimum curvature in regular grids of 100 m of K, eTh and eU. From these final grids of K, eTh and eU of the study area was generated the ternary RGB map (Figure 2).

Figure 2 - Gamma-ray spectrometric maps of the south and southwest of Minas Gerais: ternary RGB (A), K (B), eTh (C) and eU (D).

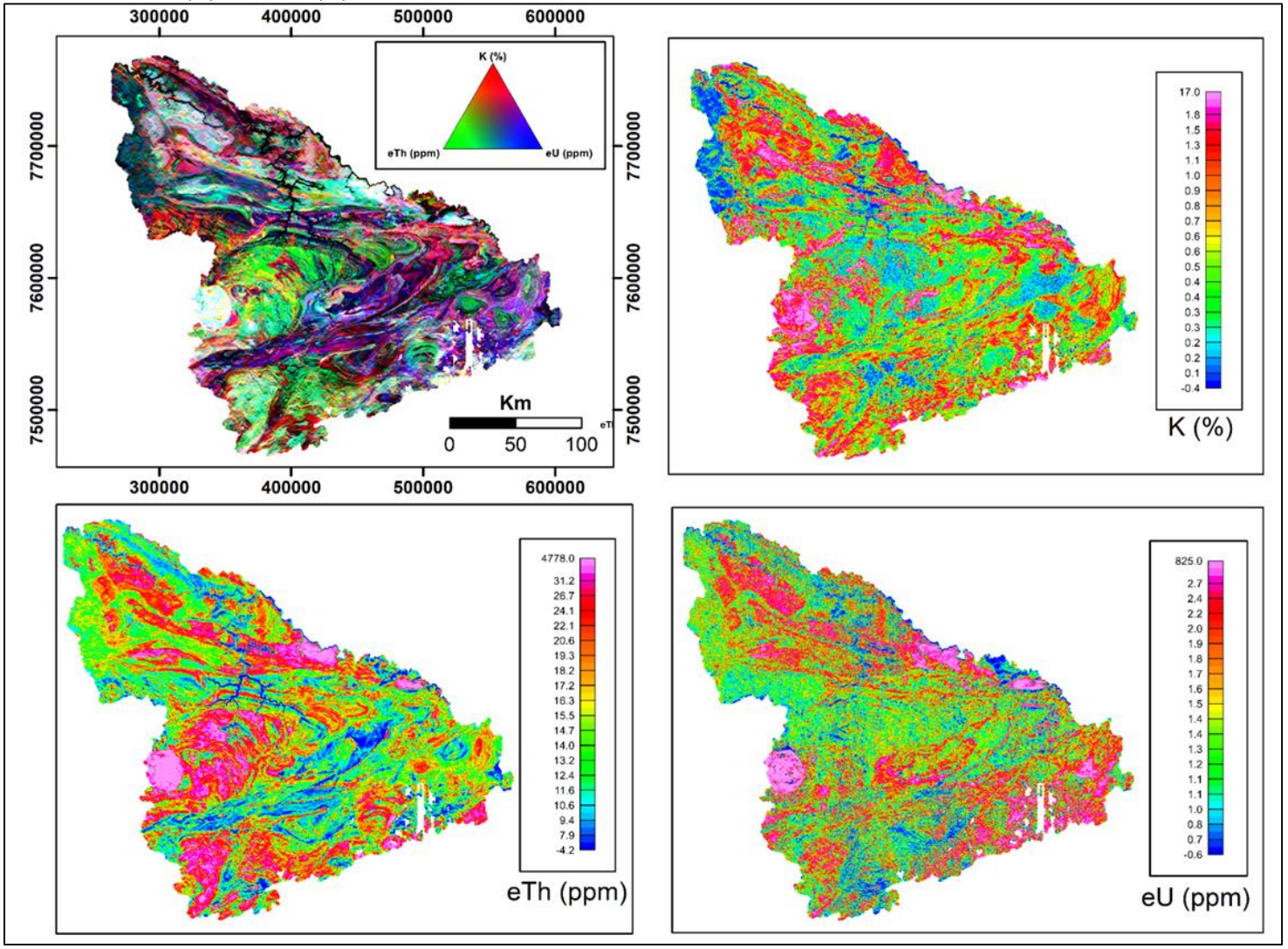

Source: Author (2021)

2.4 Soil parent material

Since gamma-ray spectroscopy was originally devoted to geological studies due to its tracer potential, in order to improve and better understand its applications in Soil Science, considerations about soil parent material rather than geology/lithology is a key point. Soil can be defined as a natural body resulting from the interaction of climate, organisms, relief and parent material acting over time (JENNY, 1941). Therefore, parent material is one of the five state factors of soil formation and, despite its weathering or consolidation conditions, it is the initial material responsible for forming soil and, consequently, has much influence on soil properties (LACOSTE; LEMERCIER; WALTER, 2011; SCHAETZL; ANDERSON, 2005).

The relationship between a soil and its parent material is not always clear. For autochthonous soils, that is, a soil developed over the geological bedrock, is easier to correlate the soil with its parent material. However, for soils with a high degree of weathering, or soils developed over superficial transported sediments, the soil parent material definition is a challenge. In the first situation, the parent material of a very weathered soil can be the residual regolith or even another soil. For those developed from superficial deposits, such as, colluvial, alluvial or aeolian sediments, the parent material not necessarily have to do with the underlying lithology or there may be more than one (KÄMPF; CURI, 2012; SCHAETZL; ANDERSON, 2005).

The knowledge of the soil parent material is very important in Soil Science, since it can drive the soil variability. There are three main parent material variables that most influence soil characteristics: consolidation degree, granulometry, and composition. Parent material consolidation degree is related with the soil profile development; unconsolidated sediments are more susceptible to experience pedological process, while consolidated rocks must be weathered to become susceptible to pedogenetic transformations (KÄMPF; CURI, 2012).

Parent material granulometry and composition affect chemical and physical soil properties, even for very weathered-leached soils. Granulometry of the parent material can be correlated with soil texture which in turn influences soil fertility, drainage, water retention capacity, among other features. Lithology or parent material composition changes soil mineralogy also influencing on soil fertility, texture, weathering susceptibility, soil profile depth and others. Weathering of felsic rocks, for example, releases low levels of Ca, Mg, Fe, and Mn, tending to kaolinite formation. Otherwise, mafic rocks release high grade of these elements supporting esmectite formation. Evidently, others state factors will influence soil

properties, thus, for the same parent material there can be different soils types (KÄMPF; CURI, 2012).

According to Lacoste, Lemercier and Walter (2011), parent material information is predominantly derived from existing geological maps. However, geological maps, predominantly those of regional scale, surface deposits may be poorly mapped, and consequently it may not be representative for soil parent material (LACOSTE; LEMERCIER; WALTER, 2011). In this sense, in Brazil new quantitative, cost-save and faster alternatives have been seek in order to improve soil parent material information and mapping more adapted to tropical conditions, for instance: a) the use of satellite multispectral analysis (MELLO et al. 2021b); b) the use of proximal sensing in soil for soil parent material tracing, since soil elemental contents (MANCINI et al. 2019; MANCINI et al. 2021) or soil magnetic susceptibility (BARBOSA et al. 2021) works as fingerprints. The use of remote sensing (passive) in the first case can be frequently limited by land cover and more suited for regional scale. Concerning proximal sensing, data is locally acquired (in-field or laboratory) and has presented great accuracy, however, when compared with remote sensing data acquisition, longer time is demanded to achieve an extensive spatial cover.

2.5 Physiographical characteristics of the study area: south region of Minas Gerais

The areas selected for this study are located in the South region of Minas Gerais state (Figure 3), accomplishing different landscapes of Red Latosols and rock outcrops (information extracted by soil mapping units polygons of the available soil information for Minas Gerais, 1:650,000). Details about environmental characteristics of the study region are presented further.

Figure 3 - Study area location showing drainage system and the main localities of the south of Minas Gerais state, southeastern Brazil.

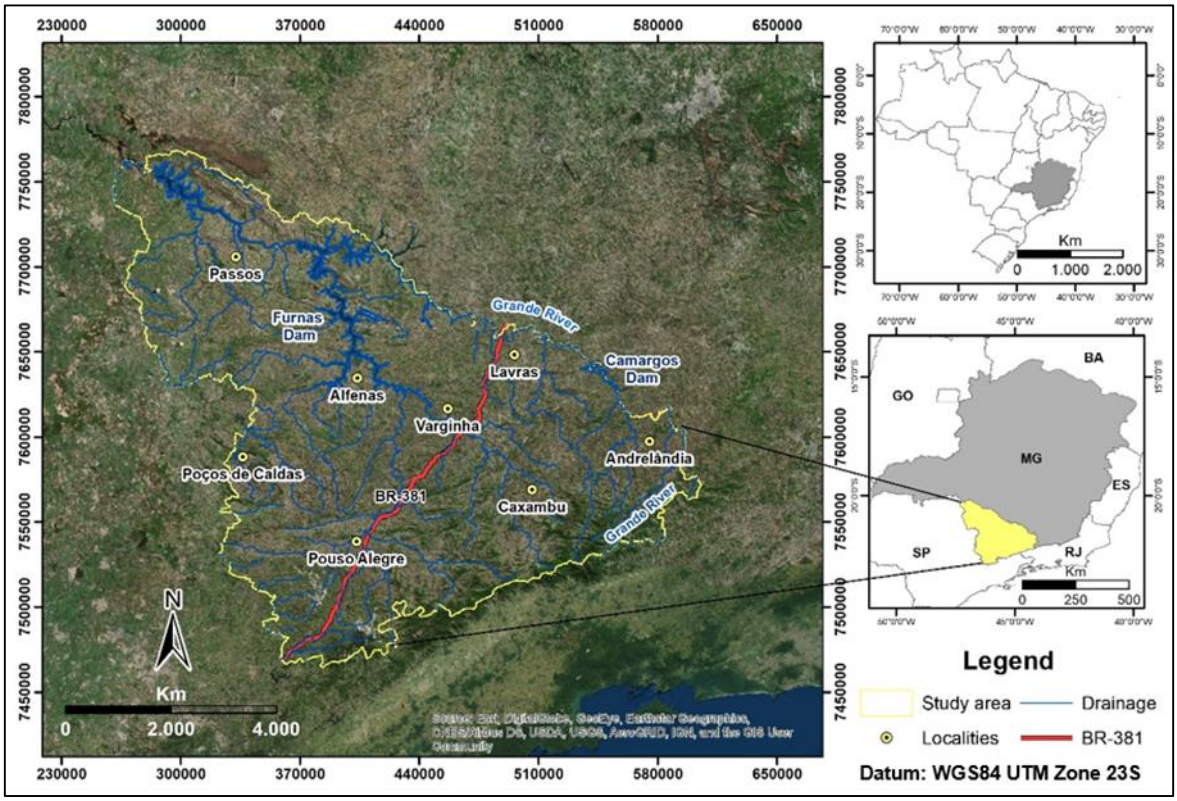

Source: Author (2021)

2.5.1 Climate

According to Köppen & Geiger climate classification system, the south of Minas Gerais presents three different climate classes: Aw, Cwa and Cwb. Aw corresponds to tropical wet and dry or savanna climate, representing less than 1% of the area. The dry (winter) and rainy (summer) seasons are strongly well defined. The average winter and summer temperatures are 22°C and 24.4°C, respectively. Cwa, subtropical dry winter, represents around 43% of the area. It has a dry winter and wet summer pattern. During the dry season (May to September), the average precipitation is less than 60 mm in at least one month. Precipitation concentrates between November to January, when precipitation is superior to 200 mm.mouth-1 and represents approximately 50% of annual precipitation. The average winter and summer temperatures are 19.7°C and 22.7°C, respectively. June presents the lowest temperatures while January, the highest. Cwb, dry-winter subtropical highland climate, corresponds approximately to 56% of the area. The dry season runs from May to August, when precipitation is inferior to 45 mm.month-1. From November to February, precipitation concentration is higher, representing around 60% of annual precipitation with rainfall superior to 200mm.month-1. The

average winter and summer temperatures are 14,3°C and 17°C, respectively (SÁ JÚNIOR, 2009).

2.5.2 Soil information

The soil survey in 1:650,000 scale of Minas Gerais is the main reference for this study (FEAM, 2010), since it is the only unified soil product for the state. Soils were classified according to Brazilian Classification System (SANTOS et al. 2018) and interpreted until suborder categorical level.

Figure 4 shows the soil map of the South region of Minas Gerais. A total of thirteen soil types were mapped, where it is possible to notice the higher variability of soil types accomplishing different weathering stages. The proportion of different soil classes in the southern region of Minas Gerais reflects the characteristic of soils in tropical environments, developed under notable and prolonged conditions of high temperatures and humidity. This combination provides a greater occurrence of soils in an advanced stage of weathering-leaching.

Following a logic of pedogenetic evolution, there is a predominance of Red Latosol which occurs in 26.5% of south Minas Gerais, followed by Red-Yellow Latosol (18.7%). The third most common soil class is the Haplic Cambisol (15%), followed by Red Argisol (14.2%), Red-Yellow Argisol (13%), Litolic Neosol (3.5%), Humic Cambisol (2.8%). The classes with the smallest territorial extension in the south of Minas Gerais are: Argiluvic Plinthosol (0.8%), Haplic Nitosol (0.6%), Melanic Gleysol, Red Nitosol and Fluvic Neosol with 0.3% and lastly Yellow Latosol (0.2%).

Figure 4 - Soil map of the South region of Minas Gerais (FEAM, 2010).

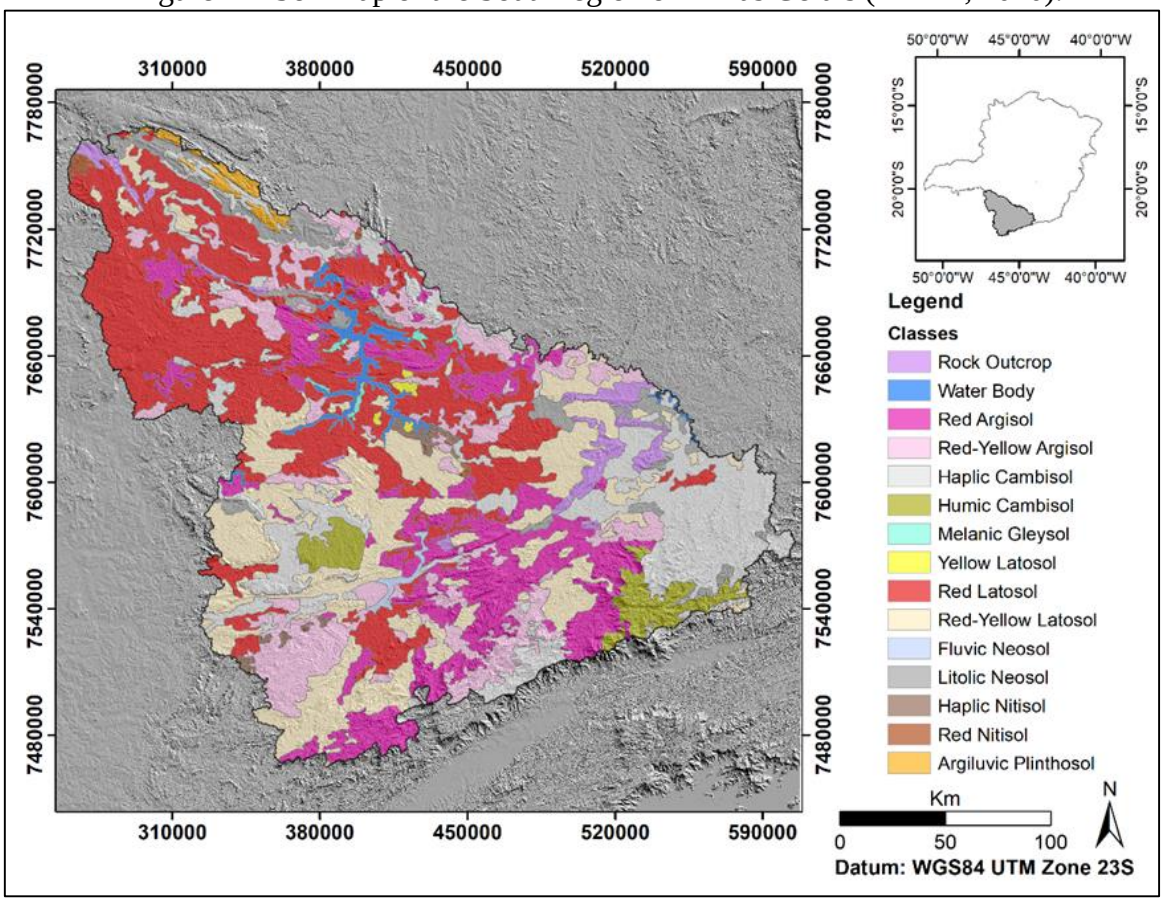

Source: Author (2021)

Red Latosol and Red-Yellow Latosol are the dominant soil classes. Such soils were classified as Latosols due to the B latosolic diagnostic horizon which occurs after any A horizon with an insignificant or null increase in clay content and a medium to very clayey texture. The mineral fraction shows a heavy weathered and leached soil: completely alteration of less stables primary minerals, silica and bases intense leaching, residual concentration of oxides, 1:1 clay minerals and quartz. Latosols present low cation exchange capacity (<17 cmolc kg-1), are usually acidic, with low bases saturation, and high aluminum saturated. Physical attributes are favorable to plant growth: they are well drained, deep, and with high water infiltration rate. Red Latosols have a Munsell color of 2.5YR or redder, if 7.5YR or yellower they are called Yellow Latosols; and classified as Red-Yellow Latosols when Munsell color is between 2.5YR and 7.5 YR. Generally, Latosols mostly occur in the smooth relief portions, above the floodplains.

In contrast, there is 2.3% of rock outcrops, characterized by IBGE (2015) as the exposure of the rocky substrate, rock slabs, or thin layer plots of soil on rocks and/or predominance of boulders with an average diameter greater than 100 cm, on the surface or in the soil mass, in such quantities that it becomes impracticable the use of agricultural machinery.

2.6 Geological Settings

In the study area, the Archean-Paleoproterozoic basement is formed by migmatized gneisses, greenstone belts, mafic-ultramafic bodies, plutons of metagabbros, metadiorites and granitoids. Overlapping the basement discordantly are Mesoproterozoic to Neoproterozoic metasedimentary sequences: São João Del Rey, Tiradentes, Carandaí, Andrelândia and Bambuí, associated with mafic to felsic meta-igneous rocks. These rocks and part of the basement were deformed and metamorphosed by the Brasiliana Orogeny on greenschist to granulite metamorphic facies. Phanerozoic record includes alkaline syenites, associated dykes and stocks, subalkaline basic dykes, sedimentary rocks of Paraná Basin and Cretaceous and Tertiary alluvial deposits. Quaternary units are represented by alluvial and colluvial sediments and talus deposits (PACIULLO et al., 1996; PEDROSA-SOARES et al., 1994; RIBEIRO et al., 2003).

I. Basement

From Archean to Paleoproterozoic age, the basement rocks in the south of Minas Gerais state are generically called the Mantiqueira Complex (POLO, 2009). It consists of TTG gneisses (trondjemito, tonalito, granodiorito), mostly ortho-derivative rocks, with amphibolites and minor ultramafic rocks. Greenstone belt type sequences are also present, such as the Fortaleza de Minas and Barbacena groups, and the Pium-hi Supergroup. They are constituted by metavulcanosedimentary associations with occurrence of intermediate-mafic-ultramafic rocks, chemical sediments, volcanoclastic, and turbiditic rocks (PACIULLO et al., 1996; POLO, 2009; RIBEIRO et al., 2003). There are also intrusions associated with reworking and partial melting of the Mantiqueira Complex. They are aged between 2.25 and 1.87 Ga, and consist of TTG complexes associated with metagabbros (POLO, 2009).

II. Proterozoic supracrustal rocks

São João Del Rei Megasequence

It is constituted by a 1000 meters thick quartzite package that outcrops in the region of São João Del Rei. Four sequences are distinguished, from the base to the top: Tiradentes, São José, Tejuco and Lenheiro (RIBEIRO et al., 2013).

The Tiradentes and São José sequences are composed of intercalations of different types of quartzites with occurrences of quartzolytic conglomerates. The Tejuco Sequence, also dominated by quartzites, presents intercalations of pelitic lenses and stromatolytic limestones.

The Lenheiros Sequence is the thickest: up to 500 meters thick. It varies from metargillites and metassiltites at the base to fine quartzites and quartzolitic conglomerates towards the top. Mafic dikes swarms up to 60 meters thick cut through the Megasequence (POLO, 2009; RIBEIRO et al., 2013).

Carandaí Megasequence

The Carandaí Megasequence occurs mainly in the region of Lavras, Ijaci and Macaia, and also towards the east and southeast of the Minas Gerais state. It outcrops in angular unconformity with quartzites of the São João Del Rei sequence or with the basement, and is covered by the Andrelândia Megasequence (POLO, 2009; RIBEIRO et al., 2013).

It is subdivided into two sequences: Barroso and Prados. The Barroso Sequence presents metadiamictites and metawackes changing gradually to carbonaceous phyllites and metamarls, followed by a thick limestone package with limestone and biotite phyllites intercalations. Prados is constituted by a broad range of metapelites at the bottom, graphite phyllites in the intermediate portion, and metapelites to phyllites at the top (POLO, 2009; RIBEIRO et al., 2013).

Andrelândia Megasequence

It outcrops throughout the Minas Gerais state southern region, both in autochthonous and allochthonous (nappes) domains (POLO, 2009). It is divided into two sequences, Carrancas and Serra do Turvo (PACIULLO et al., 2000; POLO, 2009).

Carrancas Sequence is composed of four lithofacies associations, from base to top: banded paragneisses with amphibolite intercalations (A1); banded paragneisses with amphibolite, quartzite and gray phyllite intercalations (A2); quartzite and thin intercalations of schists, both mica rich (A3); phyllites and schists with quartzite intercalations (A4) (PACIULLO et al., 1996, 2000; RIBEIRO et al., 2003).

Serra do Turvo sequence is a thick succession of three feldspathic lithological units: biotite schist of amphibolite to granulite facies (A5); chlorite biotite phyllites of green schist facies; biotite schist and gneiss with intercalations of amphibolite, gondite and siliciclastic rocks (PACIULLO et al., 1996; RIBEIRO et al., 2003).

Bambuí Group

It covers large areas of the São Francisco craton in the states of Minas Gerais, Goiás and Bahia. It is composed of a thick sequence of metasedimentary rocks of low metamorphic degree divided into the following formations: Sete Lagoas - carbonates; Serra de Santa Helena – pelites and carbonates; Lagoa do Jacaré - carbonates; Serra da Saudade - pelites; and Três Marias – arenites (IGLESIAS; UHLEIN, 2009; REIS, 2016).

III. Neoproterozoic magmatism

A series of intrusive bodies in regional scale are associated with the genesis and evolution of the Brasília and Ribeira belts (TUPINAMBÁ et al., 2007; TUPINAMBÁ; TEIXEIRA; HEILBRON, 2012). There is a wide variety of igneous bodies involving granite-gneiss complexes, syenites, granulites and migmatites. Among these bodies are: Brasília belt - Socorro Guaxupé Nappe, São José do Rio Pardo granite, Calcium-alkaline porphyritic granitoids (Socorro and Pinhal-Ipuiúna batholiths), sienitic plutons (Pedra Branca and Capituva batholiths), and late-orogenic granites; Ribeira belt – S and I types granodiorites to leucogranites (batholith of Serra dos Órgãos) with minor mafic rocks (POLO, 2009; TUPINAMBÁ et al., 2007; TUPINAMBÁ; TEIXEIRA; HEILBRON, 2012).

IV. Phanerozoic Basins

With approximately 1,500,000 km2 it covers much of the center-east portion of the South American continent. It comprises three independent sedimentation areas, up to 7,000 meters thick: Paraná Basin, Serra Geral Basin and Bauru Basin (SILVA et al., 2003).

Paraná Basin, divided in sedimentary sequences, presents intercalations of sandstones, diamictites/ conglomerates and shales. The Serra Geral Basin, outcropping in the western part of the study area, is subdivided into the Botucatu and Serra Geral formations - São Bento Group. The former is dominated by thick sandstone sequences, while the latter consists of continental flood basalts that form one of the greatest igneous provinces of the world. The Bauru Basin, divided into two groups, Caiuá and Bauru, is restricted to the NW end of the study area. It presents intercalations of sandstones, conglomerates, argillites and siltstones, with localized occurrences of volcanic rocks (SILVA et al., 2003).

V. Cretaceous Alkaline Complexes

Several intrusions of alkaline rocks occur in the southern, southeastern and central-western regions of Brazil, with a tendency to follow structural alignments of Cretaceous age (HASUI et al., 2012). They are generally circular to elliptical kilometer scale bodies that intrude, in the southern region of Minas Gerais, rocks of the Paraná Basin and of the Brasília and Ribeira belts (HASUI et al., 2012).

In the southwestern portion of the work area, the Poços de Caldas Alkaline Complex is characterized by nepheline-syenites, phonoliths, pyroclastic rocks, among other rare alkaline rocks and of restricted occurrence (SCHORSCHER; SHEA, 1992).

VI. Cenozoic and Quaternary Covers

They include a variety of recent clastic deposits resulting from weathering, erosion, transport and sedimentation processes. These include: alluvial deposits, dominant in the center-south region of the study area; clastic sediments and ferruginous laterites (PACIULLO et al., 1996; PEDROSA-SOARES et al., 1994; RIBEIRO et al., 2003).

3 GENERAL CONSIDERATIONS

Currently in Brazil, the use of gamma-ray spectrometric images is predominantly applied for mineral exploration and geological mapping through the correlation of ternary or ratio images with geological maps, seeking the identification of hydrothermal alteration zones and rock bodies delineation. To enhance its use and correctly apply in Soil Sciences (especially for Digital Soil Mapping purpose), it is important to have the knowledge of how weathering and pedogenesis processes alter the distribution of radioelements in the landscape for different lithological types. Furthermore, the integration of gamma spectrometric images with complementary data, such as digital elevation and climate models are other essential tools to get the most out of these data.

REFERENCES

ALMEIDA, F. F. M. O Cráton do São Francisco. **Revista Brasileira de Geociências**, v. 7, n. 4, p. 349–364, 1977.

ALMEIDA, F. F. M.; DE BRITO NEVES, B. B.; DAL RÉ CARNEIRO, C. The origin and evolution of the South American Platform. **Earth-Science Reviews**, v. 50, n. 1–2, p. 77–111, 2000.

BARBOSA, J. Z. et al. National-scale spatial variations of soil magnetic susceptibility in Brazil. **Journal of South American Earth Science**, v. 108, p. 103191, 2021.

BISHOP, T. F.; McBRATNEY, A. A comparison of prediction methods for the creation of field-extent soil property maps. **Geoderma**, v. 103, n. 1–2, p. 149–160, 1 set. 2001.

CHOPPIN, G. R. Humics and Radionuclide Migration. **Radiochimica Acta**, v. 44–45, n. 1, p. 23–28, 1 jan. 1988.

CODEMGE. **Levantamento Aerogeofísico**. Disponível em: <http://www.codemge.com.br/atuacao/mineracao/levantamento-aerogeofisico/>. Acesso em: 16 maio. 2019.

CODEMIG; CPRM. **Levantamento Aerogeofísico de Minas Gerais área 07: Patos de Minas - Araxá - Divinópolis**. Relatório final do levantamento e processamento dos dados magnetométricos e gamaespectrométricos, 2006. Lasa Engenharia e Prospecções S.A.

CODEMIG; CPRM. **Levantamento Aerogeofísico de Minas Gerais área 14: Poços de Caldas - Varginha - Andrelândia**. Relatório final do levantamento e processamento dos dados magnetométricos e gamaespectrométricos, 2011. Lasa Engenharia e Prospecções S.A.

CODEMIG; CPRM. **Levantamento Aerogeofísico de Minas Gerais área 15: Juiz de Fora – Cataguases - Manhuaçu**. Relatório final do levantamento e processamento dos dados magnetométricos e gamaespectrométricos, 2011. Lasa Engenharia e Prospecções S.A.

COOK, S. E. et al. Use of airborne gamma radiometric data for soil mapping. **Australian Journal of Soil Research**, v. 34, n. 1, p. 183–194, 1996.

CPRM. **Projeto Aerogeofísico São José dos Campos-Resende.** Relatório final do levantamento e processamento dos dados magnetométricos e gamaespectrométricos, 2013.

DICKSON, B. L.; SCOTT, K. M. INTERPRETATION OF AERIAL GAMMA-RAY SURVEYS-ADDING THE GEOCHEMICAL FACTORS. **AGSO JOURNAL OF AUSTRALIAN GEOLOGY & GEOPHYSICS**, V. 17, N. 2, P. 17–200, 1997.

FEAM. **MAPA DE SOLOS DO ESTADO DE MINAS GERAIS: LEGENDA EXPANDIDA**. BELO HORIZONTE: FEAM/UFV/CETEC. 2010. 49P.

FONSECA, M. A.; DARDENNE, M. A.; UHLEIN, A. FAIXA BRASÍLIA SETOR SETENTRIONAL: ESTILOS ESTRUTURAIS E ARCABOUÇO TECTÔNICO. **REVISTA BRASILEIRA DE GEOCIÊNCIAS**, V. 25, N. 4, P. 267–278, 1995.

HASUI, Y. A GRANDE COLISÃO PRÉ-CAMBRIANA DO SUDESTE BRASILEIRO E A ESTRUTURAÇÃO REGIONAL. **GEOCIENCIAS**, V. 29, N. 2, P. 141–169, 2010.

HASUI, Y. ET AL. **GEOLOGIA DO BRASIL**. SÃO PAULO: BECA, 2012.

HEILBRON, M. ET AL. CORRELATION OF NEOPROTEROZOIC TERRANES BETWEEN THE RIBEIRA BELT, SE BRAZIL AND ITS AFRICAN COUNTERPART: COMPARATIVE TECTONIC EVOLUTION AND OPEN QUESTIONS. **GEOLOGICAL SOCIETY, LONDON, SPECIAL PUBLICATIONS**, V. 294, N. 1, P. 211 LP – 237, 1 JAN. 2008.

IAEA, 2003. **GUIDELINES FOR RADIOELEMENT MAPPING USING GAMMA-RAY SPECTROMETRY DATA**. INTERNATIONAL ATOMIC ENERGY AGENCY, AUSTRIA.

IBGE. **MONITORAMENTO DA COBERTURA E USO DA TERRA DO BRASIL 2014-2016**. RIO DE JANEIRO: IBGE. 2014. DISPONÍVEL EM: <HTTPS://WWW.IBGE.GOV.BR/APPS/MONITORAMENTO_COBERTURA_USO_TERRA/V1/>. ACESSO EM: 22 JUN. 2019.

IGLESIAS, M.; UHLEIN, A. ESTRATIGRAFIA DO GRUPO BAMBUÍ E COBERTURAS FANEROZÓICAS NO VALE DO RIO SÃO FRANCISCO, NORTE DE MINAS GERAIS. **REVISTA BRASILEIRA DE GEOCIÊNCIAS**, V. 39, N. 2, P. 256–266, 2009.

IZA, E. R. H. F.; HORBE, A. M. C.; SILVA, A. M. BOOLEAN AND FUZZY METHODS FOR IDENTIFYING LATERITIC REGOLITHS IN THE BRAZILIAN AMAZON USING GAMMA-RAY SPECTROMETRIC AND TOPOGRAPHIC DATA. **GEODERMA**, V. 269, P. 27–38, 1 MAIO 2016.

JAFARI, A. ET AL. SPATIAL PREDICTION OF USDA- GREAT SOIL GROUPS IN THE ARID ZARAND REGION, IRAN: COMPARING LOGISTIC REGRESSION APPROACHES TO PREDICT DIAGNOSTIC HORIZONS AND SOIL TYPES. **EUROPEAN JOURNAL OF SOIL SCIENCE**, V. 63, N. 2, P. 284–298, 1 ABR. 2012.

JENNY, H. **FACTORES OF SOIL FORMATION: A SYSTEM OF QUANTITATIVE PEDOLOGY**. NEW YORK, NY, USA: MCGRAW-HILL BOOK CO., 1941.

KÄMPF, N.; CURI, N. FORMAÇÃO E EVOLUÇÃO DO SOLO (PEDOGÊNESE). IN: KER, J. C. ET AL. (EDS.). **PEDOLOGIA: FUNDAMENTOS**. 1. ED. VIÇOSA: SBCS, 2012. P. 207–302.

KEAREY, P.; BROOKS, M.; HILL, I. **AN INTRODUCTION TO GEOPHYSICAL EXPLORATION.** 3. ED. BLACKWELL SCIENCE, 2002.

LACOSTE, M.; LEMERCIER, B.; WALTER, C. REGIONAL MAPPING OF SOIL PARENT MATERIAL BY MACHINE LEARNING BASED ON POINT DATA. **GEOMORPHOLOGY**, V. 133, N. 1–2, P. 90–99, 1 OUT. 2011.

LANGMUIR, D. URANIUM SOLUTION-MINERAL EQUILIBRIA AT LOW TEMPERATURES WITH APPLICATIONS TO SEDIMENTARY ORE DEPOSITS. **GEOCHIMICA ET COSMOCHIMICA ACTA**, V. 42, N. 6, P. 547–569, 1 JUN. 1978.

LANGMUIR, D.; HERMAN, J. S. THE MOBILITY OF THORIUM IN NATURAL WATERS AT LOW TEMPERATURES. **GEOCHIMICA ET COSMOCHIMICA ACTA**, V. 44, N. 11, P. 1753–1766, 1 NOV. 1980.

LEMIÈRE, B. A REVIEW OF PXRF (FIELD PORTABLE X-RAY FLUORESCENCE) APPLICATIONS FOR APPLIED GEOCHEMISTRY. **JOURNAL OF GEOCHEMICAL EXPLORATION**, V. 188, P. 350–363, 1 MAIO 2018.

MACHADO, D. F. T. ET AL. TRANSFERABILITY, ACCURACY, AND UNCERTAINTY ASSESSMENT OF DIFFERENT KNOWLEDGE-BASED APPROACHES FOR SOIL TYPES MAPPING. **CATENA**, V. 182, P. 104134, 1 NOV. 2019.

MANCINI, M. ET AL. TRACING TROPICAL SOIL PARENT MATERIAL ANALYSIS VIA PORTABLE X-RAY FLUORESCENCE (PXRF) SPECTROMETRY IN BRAZILIAN CERRADO. **GEODERMA**, V. 337, P. 718-728, 2019.

MANCINI, M. ET AL. SOIL PARENT MATERIAL PREDICTION FOR BRAZIL VIA PROXIMAL SOIL SENSING. **GEODERMA REGIONAL**, V. 6, P. 00310, 2021.

MCBRATNEY, A. B. ET AL. AN OVERVIEW OF PEDOMETRIC TECHNIQUES FOR USE IN SOIL SURVEY. **GEODERMA**, V. 97, N. 3–4, P. 293–327, 1 SET. 2000.

MCBRATNEY, A. B.; WEBSTER, R. CHOOSING FUNCTIONS FOR SEMI-VARIOGRAMS OF SOIL PROPERTIES AND FITTING THEM TO SAMPLING ESTIMATES. **JOURNAL OF SOIL SCIENCE**, V. 37, N. 4, P. 617–639, DEZ. 1986.

MELLO, D. C. ET AL. APPLIED GAMMA-RAY SPECTROMETRY FOR EVALUATING TROPICAL SOIL PROCESSES AND ATTRIBUTES. **GEODERMA**, V. 381, P. 114736, 2021A.

MELLO, F. A. O. ET AL. SOIL PARENT MATERIAL PREDICTION THROUGH SATELLITE MULTISPECTRAL ANALYSIS ON A REGIONAL SCALE AT THE WESTERN PAULISTA PLATEAU, BRAZIL. **GEODERMA REGIONAL**, V. 26, P. 00412, 2021B.

METELKA, V. ET AL. AUTOMATED REGOLITH LANDFORM MAPPING USING AIRBORNE GEOPHYSICS AND REMOTE SENSING DATA, BURKINA FASO, WEST AFRICA. **REMOTE SENSING OF ENVIRONMENT**, V. 204, P. 964–978, 1 JAN. 2018.

MINTY, B. R. S. FUNDAMENTALS OF AIRBORNE GAMMA-RAY SPECTROMETRY. **AGSO JOURNAL OF AUSTRALIAN GEOLOGY & GEOPHYSICS**, V. 17, N. 2, P. 39–50, 1997.

MOONJUN, R. ET AL. APPLICATION OF AIRBORNE GAMMA-RAY IMAGERY TO ASSIST SOIL SURVEY: A CASE STUDY FROM THAILAND. **GEODERMA**, V. 289, P. 196–212, 1 MAR. 2017.

MOXHAM, R. M. NATURAL RADIOACTIVITY IN WASHINGTON COUNTRY, MARYLAND. **GEOPHYSICS**, V. 28, N. 2, P. 262–272, 7 ABR. 1963.

PACIULLO, F. V. P. ET AL. CONTRIBUIÇÃO À GEOLOGIA DO SUL DE MINAS GERAIS EDIÇÃO DAS FOLHAS 1: 50.000 ITUMIRIM, ITUTINGA, MADRE DE DEUS, LUMINÁRIAS, MINDURI E ANDRELÂNDIA. **ANUÁRIO DO INSTITUTO DE GEOCIÊNCIAS**, V. 19, P. 123–142, 1996.

PACIULLO, F. V. P. ET AL. THE ANDRELÂNDIA BASIN, A NEOPROTEROZOIC INTRAPLATE CONTINENTAL MARGIN, SOUTHERN BRASÍLIA BELT, BRAZIL. **REVISTA BRASILEIRA DE GEOCIÊNCIAS**, V. 30, N. 1, P. 200–202, 2000.

PEDROSA-SOARES, A. C. ET AL. **NOTA EXPLICATIVA DOS MAPAS GEOLÓGICO, METALOGENÉTICO E DE OCORRÊNCIAS MINERAIS DO ESTADO DE MINAS GERAIS**. BELO HORIZONTE.1994.

PIMENTEL, M. M. THE TECTONIC EVOLUTION OF THE NEOPROTEROZOIC BRASÍLIA BELT, CENTRAL BRAZIL: A GEOCHRONOLOGICAL AND ISOTOPIC APPROACH. **BRAZILIAN JOURNAL OF GEOLOGY**, V. 46, N. 1, P. 67–82, JUN. 2016.

PIRES, A. C. B.; HARTHILL, N. STATISTICAL ANALYSIS OF AIRBORNE GAMMA-RAY DATA FOR GEOLOGIC MAPPING PURPOSES: CRIXAS-ITAPACI AREA, GOIAS, BRAZIL. **GEOPHYSICS**, V. 54, N. 10, P. 1326–1332, 7 OUT. 1989.

PITELFORD, W. M.; GELDART, L. P.; SHERIFF, R. E. **APPLIED GEOPHYSICS**. NEW YORK: CAMBRIDGE UNIVERSITY PRESS, 1990.

POLO, H. J. O. **EVOLUÇÃO GEOTECTÔNICA NEO PROTEROZÓICA NA REGIÃO DE HELIODORA SUL DE MINAS GERAIS**. 2009. DISSERTAÇÃO, MESTRADO - UNIVERSIDADE FEDERAL DO RIO DE JANEIRO, RIO DE JANEIRO, 2009.

REIS, H. L. S. **NEOPROTEROZOIC EVOLUTION OF THE SÃO FRANCISCO BASIN, SE BRAZIL : EFFECTS OF TECTONIC INHERITANCE ON FORELAND SEDIMENTATION AND DEFORMATION.** 2016. TESE, DOUTORADO - ESCOLA DE MINAS, UNIVERSIDADE FEDERAL DE OURO PRETO, OURO PRETO, 2016.

RIBEIRO, A. ET AL. SÍNTESE GEOLÓGICA REGIONAL DO BLOCO OCIDENTAL, CAMPOS DAS VERTENTES E SUL DE MINAS. **GEOLOGIA E RECURSOS MINERAIS DO SUDESTE MINEIRO. PROJETO SUL DE MINAS ETAPA I**. P.51-152, 2003.

RIBEIRO, A. ET AL. U–PB LA-ICP-MS DETRITAL ZIRCON AGES OF THE SÃO JOÃO DEL REI AND CARANDAÍ BASINS: NEW EVIDENCE OF INTERMITTENT PROTEROZOIC RIFTING IN THE SÃO

FRANCISCO PALEOCONTINENT. **GONDWANA RESEARCH**, V. 24, N. 2, P. 713–726, SET. 2013.

ROUZE, G. S.; MORGAN, C. L. S.; MCBRATNEY, A. B. UNDERSTANDING THE UTILITY OF AERIAL GAMMA RADIOMETRICS FOR MAPPING SOIL PROPERTIES THROUGH PROXIMAL GAMMA SURVEYS. **GEODERMA**, V. 289, P. 185–195, MAR. 2017.

SÁ JÚNIOR, A. **APLICAÇÃO DA CLASSIFICAÇÃO DE KÖPPEN PARA O ZONEAMENTO CLIMÁTICO DO ESTADO DE MINAS GERAIS**. 2009. DISSERTAÇÃO, MESTRADO - UNIVERSIDADE FEDERAL DE LAVRAS, LAVRAS, 2009.

SANTOS, A. C. L.; MENESES, P. T. L.; NASCIMENTO, C. T. C. GAMAESPECTROMETRIA AÉREA INTEGRADA A IMAGEM SRTM (SHUTTLE RADAR TOPOGRAPHY MISSION) PARA ESTUDOS AGRÍCOLAS NA BACIA HIDROGRÁFICA DO RIO SÃO DOMINGOS: NOROESTE DO ESTADO DO RIO DE JANEIRO. **ANAIS XIV SIMPÓSIO BRASILEIRO DE SENSORIAMENTO REMOTO**, P. 443–450, 2009.

SANTOS, H. G. ET AL. **SISTEMA BRASILEIRO DE CLASSIFICAÇÃO DE SOLOS**. 5. ED., REV. E AMPL. BRASÍLIA, DF: EMBRAPA, 2018. 356 P.

SCHAETZL, R. J.; ANDERSON, S. **SOILS: GENESIS AND GEOMORPHOLOGY**. NEW YORK: CAMBRIDGE UNIVERSITY PRESS, 2005.

SCHORSCHER, H. D.; SHEA, M. E. THE REGIONAL GEOLOGY OF THE POÇOS DE CALDAS ALKALINE COMPLEX: MINERALOGY AND GEOCHEMISTRY OF SELECTED NEPHELINE SYENITES AND PHONOLITES. **JOURNAL OF GEOCHEMICAL EXPLORATION**, V. 45, N. 1–3, P. 25–51, 1 NOV. 1992.

SEME. **LEVANTAMENTO AEROGEOFÍSICO DE MINAS GERAIS ÁREA 02: PITANGUÍ – SÃO JOÃO DEL REI - IPATINGA**. RELATÓRIO FINAL DO LEVANTAMENTO E PROCESSAMENTO DOS DADOS MAGNETOMÉTRICOS E GAMAESPECTROMÉTRICOS, VOLUME I, 2006. LASA ENGENHARIA E PROSPECÇÕES S.A.

SILVA, A. J. P. DA ET AL. BACIAS SEDIMENTARES PALEOZÓICAS E MESO-CENOZÓICAS INTERIORES. IN: **GEOLOGIA, TECTÔNICA E RECURSOS MINERAIS DO BRASIL**. BRASÍLIA: CPRM, 2003. P. 55–85.

SOUZA, J. L. DE; FERREIRA, F. J. F. ANOMALIAS AEROGAMAESPECTROMÉTRICAS (K, EU E ETH) DA QUADRÍCULA DE ARARAS (SP) E SUAS RELAÇÕES COM PROCESSOS PEDOGENÉTICOS E FERTILIZANTES FOSFATOS. **REVISTA BRASILEIRA DE GEOFÍSICA**, V. 23, N. 3, P. 251–274, SET. 2005.

TAYLOR, M. J. ET AL. RELATIONSHIPS BETWEEN SOIL PROPERTIES AND HIGH-RESOLUTION RADIOMETRICS, CENTRAL EASTERN WHEATBELT, WESTERN AUSTRALIA. **EXPLORATION GEOPHYSICS**, V. 33, N. 2, P. 95–102, 6 JUN. 2002.

THIESSEN, K. ET AL. MODELLING RADIONUCLIDE DISTRIBUTION AND TRANSPORT IN THE ENVIRONMENT. **ENVIRONMENTAL POLLUTION**, V. 100, N. 1–3, P. 151–177, 1 JAN. 1999.

TUPINAMBÁ, M. ET AL. GEOLOGIA DA FAIXA RIBEIRA SETENTRIONAL: ESTADO DA ARTE E CONEXÕES COM A FAIXA ARAÇUAÍ. **GEONOMOS**, V. 15, N. 1, P. 67–79, 16 FEV. 2007.

TUPINAMBÁ, M.; TEIXEIRA, W.; HEILBRON, M. EVOLUÇÃO TECTÔNICA E MAGMÁTICA DA FAIXA RIBEIRA ENTRE O NEOPROTEROZOICO E O PALEOZOICO INFERIOR NA REGIÃO SERRANA DO ESTADO DO RIO DE JANEIRO, BRASIL. **ANUÁRIO DO INSTITUTO DE GEOCIÊNCIAS**, V. 35, N. 2, P. 140–151, 2012.

VASCONCELLOS, R. M. ET AL. **GEOFÍSICA EM LEVANTAMENTOS GEOLÓGICOS NO BRASIL**. RIO DE JANEIRO: CPRM. 172P. 1994.

WILFORD, J. A WEATHERING INTENSITY INDEX FOR THE AUSTRALIAN CONTINENT USING AIRBORNE GAMMA-RAY SPECTROMETRY AND DIGITAL TERRAIN ANALYSIS. **GEODERMA**, V. 183–184, P. 124–142, 1 AGO. 2012.

WILFORD, J. R.; BIERWIRTH, P. N.; CRAIG, M. A. APPLICATION OF AIRBORNE GAMMA-RAY SPECTROMETRY IN SOIL/REGOLITH MAPPING AND APPLIED GEOMORPHOLOGY. **AGSO JOURNAL OF AUSTRALIAN GEOLOGY AND GEOPHYSICS**, V. 28, N. 16, P. 201–216, 1997.

YOUSSEF, M. A. S. RELATIONSHIPS BETWEEN GROUND AND AIRBORNE GAMMA-RAY SPECTROMETRIC SURVEY DATA, NORTH RAS MILLAN, SOUTHERN SINAI PENINSULA, EGYPT. **JOURNAL OF ENVIRONMENTAL RADIOACTIVITY**, V. 152, P. 75–84, 1 FEV. 2016.

SECOND PART

ARTICLE: EVALUATION OF AIRBORNE GAMMA-RAY SPECTROMETRY IN CONTRASTING LANDSCAPES UNDER TROPICAL CONDITIONS

ABSTRACT

Airborne gamma-ray spectroscopy detects the natural gamma radiation of the radionuclides uranium (U238), thorium (Th232), and potassium (K40) in the upper 30 cm of the Earth's surface, used to infer U, Th and K concentrations, respectively. There is a large cover of such radionucleotides in Brazil providing a continuous coverage, whose values are driven by mineralogy and geochemistry of rocks, soils, and sediments. Considering the great potential of airborne gamma-ray radiometric to trace soil parent material, and the scarcity of studies under tropical conditions, this work aimed to explore the relationship among %K, eTh and eU with contrasting conditions of soil, geology, relief, and climate in the south of Minas Gerais state. The specific objectives were: i) to understand the influence of environmental attributes on the dynamics of the radionucleotides; ii) to understand how pedogenesis changes the radioelements signature in tropical landscapes; iii) to evaluate the potential of gamma spectrometric images in mapping soil parent material for regional studies. Seeking contrasting conditions of weathering stages and different geologies, representative areas containing rock outcrops and Red Latosols in different rock groups of pedopsamitic, poor pedopelitic, pedomafic and pedogneissic were selected. Airborne gamma-ray data were obtained from aerogeophysical surveys. Individual K, eTh, eU channels, the ratios eTh/K, eU/K, U/Th and the F Parameter were processed, interpolated and corrected. K and F parameter stand out as a tracer of different rock groups even in landscapes with different development, being positively correlated with topographic parameters such as texture, slope, and terrain ruggedness index. Besides terrain, Red Latosols were also positively correlated with paleoclimate (annual total precipitation of 6,000 years ago), in accordance with their polygenetic nature. Gamma spectrometry images must be analyzed in the spatial context in which they occur, since the relationships between radionucleotides and environment might be complex.

Keywords: Airborne gamma-ray spectroscopy. Contrasting landscapes. Tropical environment.

1 INTRODUCTION

There is a large cover of airborne gamma-ray spectroscopy surveys in Brazil, accomplishing 43% of the territory (CPRM, 2020). The focus of such great effort was mineral exploration and geological mapping, since geological features such as bodies, structures and mineral deposits can be inferred in depth through interpretations and modeling of gamma-rays naturally emitted form earth´s surface (FORTIN; HOVGAARD; BATES, 2017) in the upper 30 cm. Gamma-ray spectrometry detects the natural gamma radiation emitted by the disintegration of potassium (40K) and series of uranium (238U) and thorium (232Th) radioisotopes. Thus, these are used to infer K, U and Th concentrations (MINTY, 1997). Potassium concentration is directly measured by the gamma-ray photons emitted by decay of 40K to 40Ar. The abundance of U and Th are measured counting distinct emission peaks of their daughter nuclides 214Bi and 208Tl, respectively. For this reason, U and Th are expressed as equivalent eU and eTh indicating that their concentrations are inferred from daughter elements (COOK et al., 1996; DICKSON; SCOTT, 1997; MINTY, 1997; WILFORD; BIERWIRTH; CRAIG, 1997).

Regarding the pattern of occurrence of K, the most abundant radioisotope in Earth's crust, it is found predominantly in alkali primary minerals such potassic feldspars and micas (e.g. biotite and muscovite), and it is absent on mafic minerals. Hence, K has relatively high concentration on felsic rocks, but low and very low on mafic and ultramafic rocks, respectively. During the weathering of K-bearing primary minerals the potassium released is adsorbed in the formation of K-bearing clay minerals as illite, montmorillonite, and in less amounting kaolinite. K is a mobile and soluble element on weathering conditions, and the adsorption of K by clays is reflected in the low concentrations of K in sea water (DICKSON; SCOTT, 1997; WILFORD; BIERWIRTH; CRAIG, 1997). U and Th are relative rare element on Earth's crust. Uranium occurs in rocks: i) as oxide and silicate minerals of uraninite and uranothorite, mainly in monazite, xenotime and zircon; ii) as trace elements in other rock-forming minerals; iii) along grain boundaries as oxides or silicates (DICKSON; SCOTT, 1997). Zircon and monazite are the only U-bearing minerals that remain stable during weathering. The U released by U-bearing minerals weathering may be retained in authigenic iron oxides and clay minerals, or precipitated under reducing conditions (DICKSON; SCOTT, 1997). Th may be present in allanite, monazite, xenotime, and zircon at levels higher than 1000 ppm or as trace element in other rock forming minerals. Monazite and zircon are the major Th-bearing minerals, and due to their stability, they may accumulate in heavy mineral sand deposits. Th released by weathering may be

retained onto Fe or Ti oxides or hydroxides, and clays. As U, Th may be absorbed onto iron oxides and colloidal clays (DICKSON; SCOTT, 1997).

Most of gamma-rays pass through moderately dense vegetation, allowing direct measurement of soil geochemistry without the masking effect of crops or trees that can limit the use of other remotely sensed datasets such as optical sensors (WILFORD; MINTY, 2007). As a remote sensing product, there is the advantage of continuous coverage of the structure and composition of the subsurface over large areas in a relatively short time (FORTIN; HOVGAARD; BATES, 2017). Thus, the distinction of geological materials nature is based on the assumption that different rock types are composed of certain amounts of rock-forming minerals, containing specific quantities of radioactive elements (YOUSSEF, 2020). Furthermore, the intensity of gamma-ray radiation is govern by mineralogy and geochemistry of rocks, soils, sediments, (WILFORD; BIERWIRTH; CRAIG, 1997; DICKSON; SCOTT, 1997; MINTY, 1997), increasing their potential use and tracing the link between surface expression of geological features and their geochemical composition (FORTIN; HOVGAARD; BATES, 2017). Aspects related to soil pedogenesis, weathering-leaching intensity, processes related to landscape formation and evolution are also key points that govern K, U and Th dynamics.

Radioelements contents on regolith or soil can differ considerably from their source rocks due to textural and geochemical reorganization in the weathering profile (WILFORD; BIERWIRTH; CRAIG, 1997). Weathering might result on loss of K in all rocks types. For felsic rocks there are also loss of U and Th. During initial weathering, intermediate, mafic and ultramafic rocks show less change in radioelements content, but pedogenetic process can produce soils with relatively higher concentration of U and Th, increased with basicity of the rock. Then, soils derived from different lithological units can show similar radioelement content needing additional data sets and field checking for confusing signatures and anomalous areas (DICKSON; SCOTT, 1997). To achieve an assertive interpretation of the radioactive signatures of %K, eTh and eU in tropical and ancient landscapes must take into account, aspects such as: i) U, Th, K have different mobility and weathering and pedogenesis can change radionuclide concentration and distribution in the environment; ii) U, Th, K spatial distribution prediction might be improved by using relief and climate data; iii) correlation of radionuclides content with soil parent material must consider these landscapes attributes.

Considering the great potential of airborne gamma-ray radiometric to trace soil parent material, and the scarcity of studies under tropical conditions, this work aimed to explore the relationship among %K, eTh and eU with contrasting conditions of soil, geology, relief, and

climate in the south of Minas Gerais state. Representative areas containing rock outcrops and Red Latosols were selected, since they represent the most contrasting conditions of weathering stage. The specific objectives were: i) to evaluate the influence of environmental attributes on the dynamics of the radionucleotides; ii) to evaluate how pedogenesis changes the radioelements signature in tropical landscapes; iii) to evaluate the potential of gamma spectrometric images in mapping soil parent material for regional studies.

2 MATERIALS AND METHODS

2.1 Study area

This study comprises landscapes in the south region of Minas Gerais State, southeastern Brazil. To the south, it borders the states of São Paulo and Rio de Janeiro; to the north, the Grand River limits the area from west to east (Figure 1).

Figure 1 - Study area location

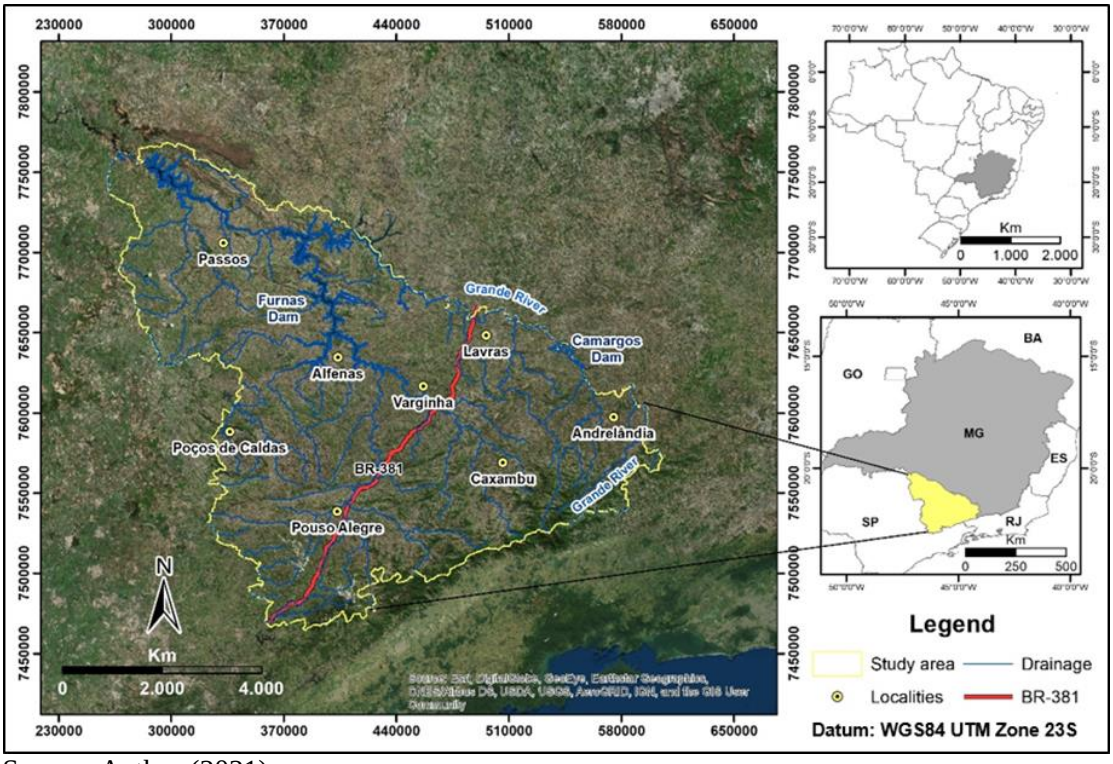

Source: Author (2021)

According to CPRM (2010), most of the area is included in the geomorphological domain of denudation units in crystalline and sedimentary rocks, with a complex physiography

composed of mountains, dissected hills, and lower slopes of surrounding mountains. Geology is quite complex, encompassing Mantiqueira, Tocantins, Paraná and São Francisco structural provinces. It comprises basement rocks represented by Archean to Paleoproterozoic TTG gneisses, granitoid intrusions and greenstone belt type sequences; Proterozoic supracrustal rocks – São João Del Rei, Carandaí, Andrelândia megasequences, and the Bambuí group; Neoproterozoic magmatism related to the evolution of Neoproterozoic magmatic arcs (Brasília and Ribeira belts); Phanerozoic units divided in three main basins – Paraná, Serra Geral and Bauru – with thick sedimentary and flood basalts sequences; and Cretaceous Alkaline Complexes (PACIULLO et al., 1996; PEDROSA-SOARES et al., 1994; RIBEIRO et al., 2003).

2.2 Representative landscapes selection

Polygons containing representative landscapes were pre-defined based on the following characteristics of the south region of Minas Gerais state, available soil and geological maps, supported by specialized literature:

a) Based on the soil-landscape relationship of the region, the greatest contrast is found by comparing the highly weathered soils of the tropics – Red Latosols – with the less developed pedoenvironment composed by rock outcrops. The soil mapping unit polygons from the soil survey in 1:650,000 scale (FEAM, 2010) was applied, since it is the only unified soil map product of the State currently. Soils were interpreted until suborder categorical level according to Brazilian Soil Classification System (SANTOS et al., 2018). In the case of Red Latosols, only polygons that contained a complete soil profile description within were chosen in order to reduce uncertainty avoiding those soil map units that could be generalization of mapping.

b) In the both landscapes above mentioned, it was also sought contrasts provided by the underlying or exposed rock grouping. Based on extensive soil surveys developed in Brazil, Resende (1982), Muggler, Lopes and Rezende (1990), and Resende et al. (2019) suggested a grouping of rocks for pedological purposes, based on the assumption that petrological criteria itself might not correlates well with soil forming aspects. Thus, the components of geological map of Minas Gerais scale 1:1,000,000 (CPRM, 2003) were grouped based on such concepts.

Figure 2 A shows further details about the definition of the target landscapes for the analysis and Figure 2 B presents the map with the location of the rock outcrops and Red Latosol for the following rock groupings: pedopsamitic, poor pedopelitic, pedomafic and pedogneissic. Pedopsamitic grouping includes cemented quartz rocks with predominantly sand-sized particles. Poor pedopelitic comprises rocks whose main original components are the clayey and

silt fraction (aluminum rich components) and generally have planar oriented structures. Pedomafic grouping include rocks of mafic composition such as basalts; and the pedogneissic grouping is mainly composed by leuco/mesocratic gneisses and biotite-schists (RESENDE, 1982; MUGGLER; LOPES; REZENDE, 1990; RESENDE et al., 2019). Table 1 presents the predominant lithotypes, geological units, tectonic domains, and geological ages of the selected landscapes.

Figure 2 - A) Methodology used to select the landscapes targeted by the study. B) Map of selected landscapes for statistical analysis.

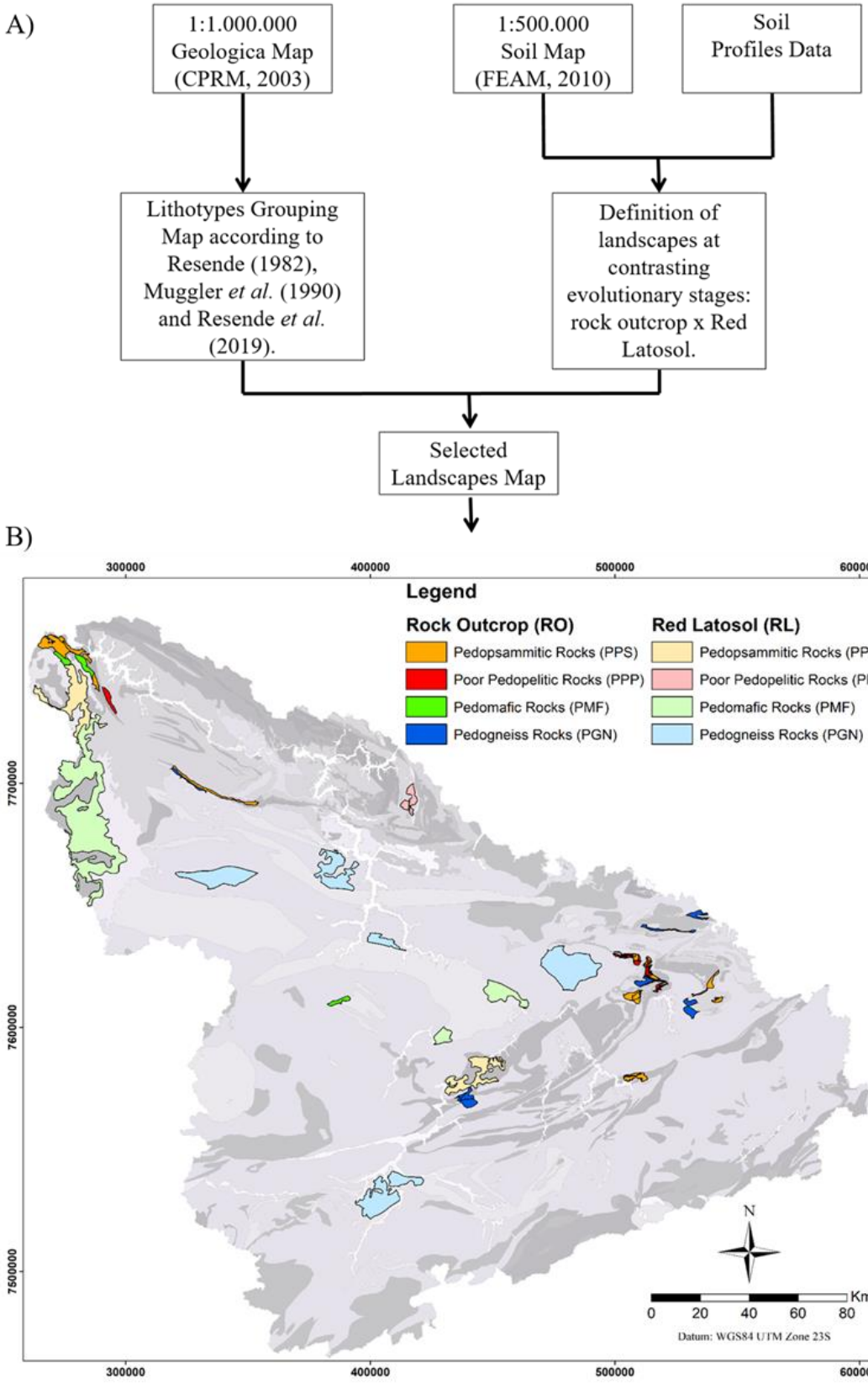

Source: Author (2021)

Table 1 - Description of predominant lithotypes and geological features of selected landscapes.

Landscapes	Predominant Lithotypes	Geological Units	Tectonic Domains	Age
Pedopsamitic-rock outcrop	Micaceous quartzite; Quartzite; Sandstone; Metagraywacke	Canastra Group; Araxá Group; Botucatu Formation; Andrelândia Group	Rift Basin; Forearc basin with ophioliths; Paraná intracontinental basin; Passive margin basin	Mesozoic; Neoproterozoic
Pedopsamitic-Red Latosol	Sandstone; Metagraywacke	Botucatu Formation; Andrelândia Group	Paraná intracontinental basin; Passive margin basin	Mesozoic; Neoproterozoic
Poor Pedopelitic-rock outcrop	Phyllite and gray schist; chlorite-schists, biotite-schist, graphite-schist, talc-schist	Andrelândia Group; Araxá Group	Passive margin basin; Forearc basin with ophioliths	Neoproterozoic
Poor Pedopelitic-Red Latosol	Pelitic-sandy rhythmite association	Pium-hi Supergroup, Turbidite sequence	Greenstone belt complexes	Archean
Pedomafic-rock outcrop	Basalt; metaultramafics	Serra Geral Formation; Varginha-Guaxupé Complex	Basic continental volcanism of Paraná Basin; Varginha nappe magmatic arc	Cretaceous; Neoproterozoic
Pedomafic-Red Latosol	Basalt; metaultramafics	Serra Geral Formation; Varginha-Guaxupé Complex	Basic continental volcanism of Paraná Basin; Varginha nappe magmatic arc	Cretaceous; Neoproterozoic
Pedogneissic-rock outcrop	TTG-type banded orthogneisses; Biotite schist/coarse gneiss	Mantiqueira Complex; Andrelândia Group; Carandaí Group; Campos Gerais Complex	TTG orthogneisses complexes; Passive margin basin; orogenic basin; Caating-Lamim Gneiss	Paleoproterozoic; Neoproterozoic; Mesoarchean
Pedogneissic-Red Latosol	Grenade-Kyanite-K-feldspar gneiss and Biotite schist/coarse gneiss; TTG-type banded orthogneisses; migmatitic orthogneiss	Andrelândia Group; Campos Gerais Complex; Varginha-Guaxupé Complex	Passive margin basin; TTG complexes; Type I and C granites from the Varginha nappe magmatic arc	Neoproterozoic; Mesoarquean

Legend: TTG = trondhjemite-tonalite-granodiorite.

2.3 Airborne gamma-ray data

2.3.1 Airborne gamma-ray spectrometry survey

Airborne gamma-ray data were obtained from aerogeophysical surveys coordinated by Companhia de Desenvolvimento de Minas Gerais (Codemig) and Serviço Geológico do Brasil (CPRM). From 2001 to 2013, Codemig developed an extensive geophysical survey program in Minas Gerais (CODEMGE, 2013), comprising part of the projects 2, 7, 14 and 15. Aerogeophysical survey of the south part of the study area (São José dos Campos – Resende Project) was coordinated by CPRM (Figure 3).

Figure 3 - Aerogeophysical surveys in Minas Gerais state, and interested areas leaded by Codemig (areas 2, 7, 15, and 15) and CPRM (São José dos Campos – Resende Project).

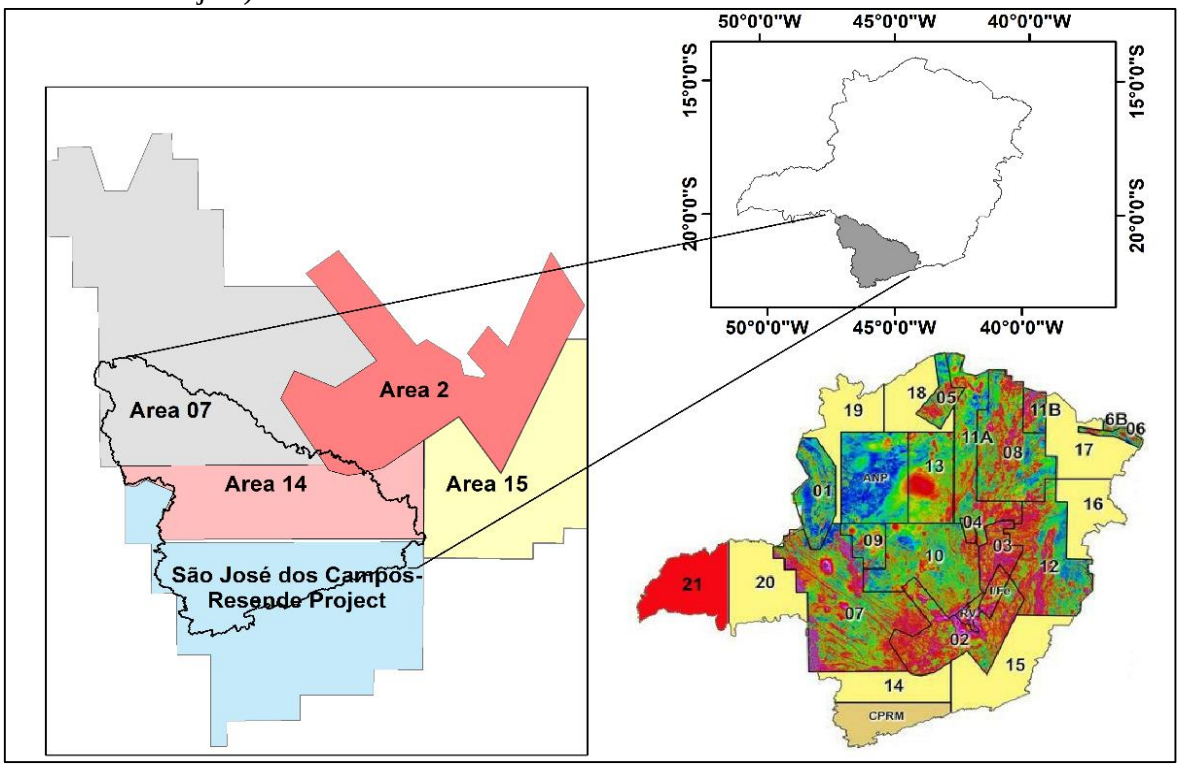

Source: Author (2021)

Prospecting and data processing of areas 02, 07, 14 and 15 were conducted by Lasa Engenharia e Prospecções S.A (CODEMIG; CPRM, 2006, 2011). The São José dos Campos-Resende Aerogeophysical Project (Area SJC-R), which covers the south of the study area was executed and processed by Microsurvey Aerogeofísica e Consultoria Científica LTDA from 2010 to 2013 (CPRM, 2013). The Table 2 below summarizes technical features of the aerial surveys.

Table 2 - Technical features of the aerial surveys that encompass the study area.

Survey technical features	Area 02 (west)	Area 07	Area 14	Area 15	Area SJC-R
Flight line direction	N30E	N-S	N-S	N-S	N-S
Flight line spacing	250 m	400 m	500 m	500 m	500 m
Control lines direction	N60W	E-W	E-W	E-W	E-W
Control lines spacing	2500 m	8000 m	10000 m	10000 m	10000 m
Interval between consecutive measurement	1.0 s	1.0 s	1.0 s	1.0 s	1.0 s
Average flight height	100 m	100 m	100 m	100 m	100 m
Average flight speed	200 km/h	280 km/h	263 km/h	242 km/h	265km/h
Distance between collected data	80 m	78 m	73 m	67 m	75 m
Gamma-ray spectrometer	Exploranium GR-820	Exploranium GR-820	Exploranium GR-820	Exploranium GR-820	Exploranium GR-820; Pico Envirotec GRS410; Radiation Solutions INC RS-500

The number of gamma-rays recorded is proportional to the concentration of the radioelements in the source, and the energies of the gamma-rays can be used to determine the composition of the source isotopes (WILFORD; MINTY, 2007). The data obtained were submitted to standard processing and corrections including: dead time effect, calculation of

effective flight height, Compton scattering, altimetric correction, background radiation associated with the aircraft cosmic radiation, and atmospheric radon following the procedure recommended by the International Atomic Energy Agency (CODEMIG; CPRM, 2006, 2011; CPRM, 2013). The procedures are carried out in the OASIS MONTAJ software. The data used for interpolation were provided in table format in the extensions XYZ or GDB.

2.3.2 Airborne gamma-ray images

The software OASIS MONTAJ version 9.7 (Seequent company) was used for data interpolation, applying the statistical technique of minimum curvature generating a final map in 100 m regular grids. Visual inspection of K, eTh and eU grids showed few pixels of negative concentrations for all channels, mainly at the edges of the projects. To smooth out these negative values, the total area grids were converted on GDB (sample a grid tool) and using a mask tool the negative values of each channel were replaced by zero and again interpolated by minimum curvature in regular grids of 100 m of K, eTh and eU. The images generated from interpolations include individual K, eTh, eU channels, the ratios eTh/K, eU/K, U/Th and the F Parameter (GNOJEK; PRICHYSTAL, 1985; RIBEIRO; MANTOVANI; LOURO, 2015). Geosoft extension for ArcGIS version 10.0 of ESRI allowed the rasterization of airborne geophysical images.

2.4 Topographic and climatic data

Topographic and climatic data were acquired or calculated in Geographical Information System, in order to assess their influence on radionucleotides values (Table 3). Terrain variables were derived from the Digital Elevation Model (DEM) from the Shuttle Radar Topography Mission (SRTM) with a spatial resolution of 90m (available at https://www.cnpm.embrapa.br/projetos/relevobr/download/mg/mg.htm). After operations to become the DEM hydrologically consistent, terrain variables were calculated by ArcGIS and SAGA GIS 12 software (CONRAD et al., 2007).

Climate data was acquired through the WorldClim website, a free set of global climate layers with a spatial resolution from 1 to 5 km. Climate grids include current and estimated data of precipitation for the Middle Holocene Period (6,000 years ago), Last Glacial Maximum

(about 22,000 years ago), and Last Interglacial Period (between 120,000 and 140,000 years ago).

Tabela 3 - Sources and resolution of topographic and climatic data

Raster layer	Resolution	Source
Topography		
Digital Elevation Model (MDE)	90m	SRTM
Slope	90m	CONRAD (2001)
Topographic Wetness Index (TWI)	90m	CONRAD (2003)
Terrain Ruggedness Index (TRI)	90m	CONRAD (2010)
Texture	90m	CONRAD (2012)
Relative Slope Position (Relative_S)	90m	BOEHNER, CONRAD (2008)
Climate		
Annual Total Precipitation (bio 12)	1 km	XU; HUTCHINSON (2013)
Annual Total Precipitation 6.000 years (bcmidbi12)	1 km	TAYLOR; STOUFFER; MEEHL (2012)
Annual Total Precipitation 6.000 years (ccmidbi12)	1 km	
Annual Total Precipitation 6.000 years (cnmidbi12)	1 km	
Annual Total Precipitation 6.000 years (hemidbi12)	1 km	
Annual Total Precipitation 6.000 years (hgmidbi12)	1 km	
Annual Total Precipitation 6.000 years (ipmidbi12)	1 km	
Annual Total Precipitation 6.000 years (memidbi12)	1 km	
Annual Total Precipitation 6.000 years (mgmidbi12)	1 km	
Annual Total Precipitation 6.000 years (mrmidbi12)	1 km	
Annual Total Precipitation 20.000 years (cclgmbi12)	5 km	
Annual Total Precipitation 20.000 years (melgmbi12)	5 km	
Annual Total Precipitation 20.000 years (mrlgmbi12)	5 km	
Annual Total Precipitation 120.000 years - model BP (ligbio12)	1 km	OTTO-BLIESNER et al. (2009)

2.5 Data analysis

Figure 4 presents the complete flowchart of the statistical analysis procedures. In order to understand how gamma-ray data varies within rock outcrops and Red Latosols domains over different type of rocks, different boxplots containing such variation were created for pixel values of K, eTh, eU and ratios. In addition to the descriptive statistical analyses, principal component analysis (PCA) biplot was performed to understand the importance and intercorrelation of topographic, climate, and paleoclimate data with the radionucleotides. The PCAs were created in FactoMineR package (HUSSON; LE; JÉRÔME, 2017) of R software (R Development Core Team).

PCA is an exploratory multivariate analysis statistical method that allows describing and summarizing a large set of data in different measurement units, facilitating the correlation and interpretation of data (HUSSON; LE; JÉRÔME, 2017). For each PCA, the circle of eigenvectors of the variables for the first two components was constructed, represented by the x and y axes (respectively, first and second axes). The components are built by combining the correlation between the variables and estimated in order to contain as much information as possible in relation to the contribution to the total variation of the data, considering a descending order of relevance. Eigenvectors are the results of the weights of each variable in each component (axes). Such weights work as a measure of the relative importance of each variable in relation to the main components and the respective signs, positive or negative, indicate direct or inversely proportional relationships (KENT; COKER, 1992).

Figure 4 - Flowchart of the procedures used to compose the database and the statistical analyzes performed. PCA – principal component analysis.

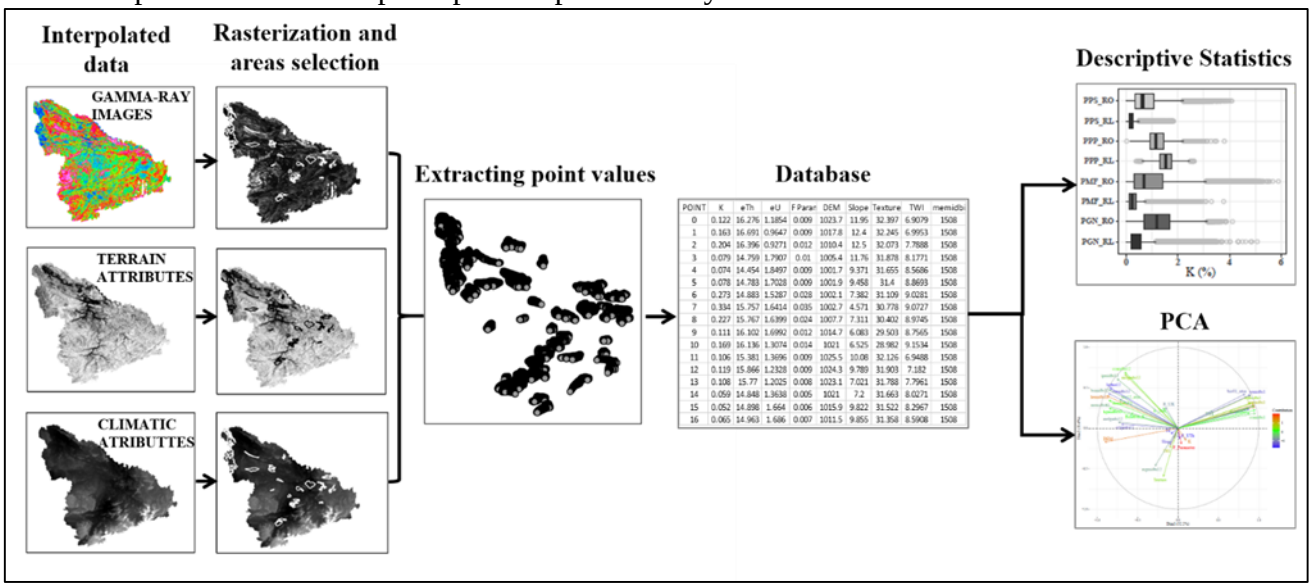

Source: Author (2021)

3 RESULTS AND DISCUSSIONS

3.1 Analysis of gamma-ray spectrometric contents in the different landscapes

Table 4 shows the descriptive statistics of airborne gamma-ray spectrometric data of RO (39.954 pixels) and RL (193.506 pixels). Higher variances and coefficient of variations, as well as great coincidence of data amplitudes can be observed. The RO presented relatively lower

contents (mean ± standard deviation) of eTh (14.34 ppm ± 6.03 ppm), and higher contents of eU (1.54 ppm ± 0.81 ppm) and K (1.01% ± 0.74%) when compared to LV. The later, in turn, presented eTh contents of 15.98 ppm ± 4.92 ppm, eU of 1.45 ppm ± 0.43 ppm and K of 0.39% ± 0.40%. K, U and Th behave differently from one another during bedrock weathering and pedogenesis. K was three times lower in RL than RO, due to its higher solubility causing higher leaching rates from the soil profile throughout the time (CURTIS, 1976; DICKSON; SCOTT, 1997; WILFORD; BIERWIRTH; CRAIG, 1997; TAYLOR; EGGLETON, 2001; WILDFORD; MINTY, 2007; MELO et al., 2021), also exerting influence on those ratios that contain (especially F parameters).

In contrast, eU and eTh generally tends to be associated with relatively stable constituents of soils and remain in soils during weathering and pedogenesis, but only a slight difference of mean values of eU and eTh was noticed by comparing RL and RO, since their mobility and re-distribution is often complex (WILFORD, 2012). Thus, in order to better understand radioelements concentration, their content in different types of rocks as well as their behavior after mineral releasing must be considered. In this sense, the values radioelements and ratios distributions of RO and RL formed by different rock grouping are presented in Figure 5.

Table 4 - Descriptive statistics of gamma spectrometric values in the domains of rock outcrops and Red Latosols.

Gamma-ray product	Mean	Standard deviation	Coefficient of variation	Variance	Minimum	Median	Maximum
Rock Outcrop							
eTh (ppm)	14.34	6.03	0.42	36.34	1.82	13.33	68.00
eU (ppm)	1.54	0.81	0.52	0.65	0.00	1.36	6.98
F parameter	0.12	0.10	0.88	0.01	0.00	0.09	1.11
K (%)	1.01	0.74	0.73	0.55	0.01	0.87	5.89
Th/K	30.03	55.71	1.86	3103.82	1.20	14.94	999.56
U/K	3.04	5.45	1.79	29.73	0.00	1.67	161.69
U/Th	0.11	0.05	0.44	0.00	0.00	0.11	0.93
Red Latosol							
eTh (ppm)	15.98	4.92	0.31	24.18	3.77	15.04	54.74
eU (ppm)	1.45	0.43	0.30	0.19	0.00	1.43	4.35
F parameter	0.04	0.04	1.07	0.00	0.00	0.02	0.83
K (%)	0.39	0.40	1.02	0.16	0.01	0.26	5.08
Th/K	90.01	107.23	1.19	11497.51	2.86	57.89	999.92
U/K	8.52	11.06	1.30	122.28	0.00	5.28	179.41
U/Th	0.10	0.03	0.34	0.00	0.00	0.09	0.35

Figure 5 - Boxplots for the following parameters considering the selected landscapes: K (A), eTh (B), eU (C), Th/K (D); U/K (E), U/Th (F) and F parameter (G).

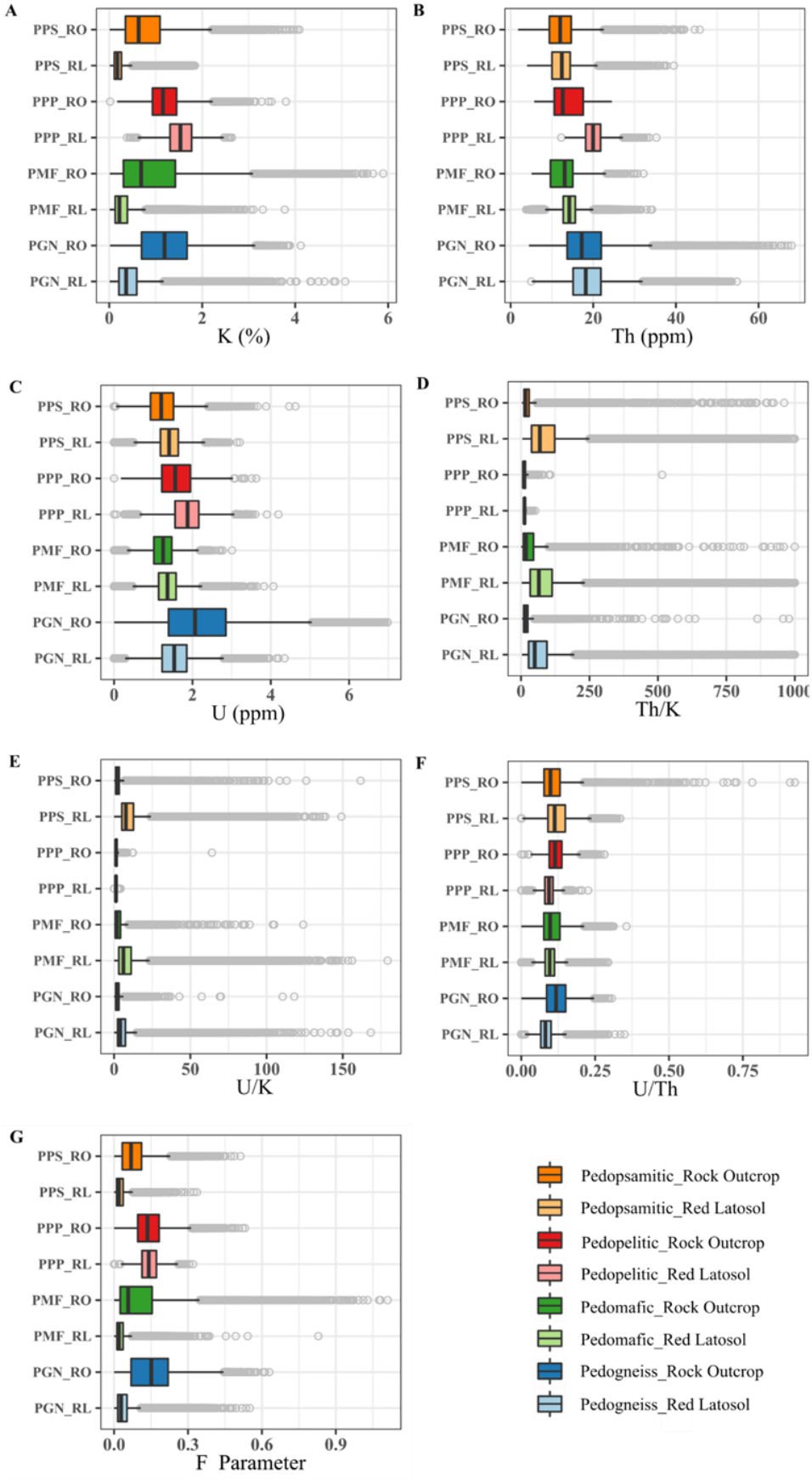

Source: Author (2021)

Although outliers were previously removed, there is still an overlapping of minimum and maximum values, probably due to the great generalization (coarse scale) of the mapping units of soil survey or geological maps, or due to artefacts of data interpolation. Nevertheless, it is possible to notice distinction of radioelements in the different landscapes by analyzing the lower, middle and upper quartiles of boxplots (main landscape trace values once they contain higher concentration of data).

The ratios Th/K, U/K, U/Th promoted only slight distinctions among rock groupings, denoting their low tracer potential. Such ratios have been calculated to enhance contrasts (DICKSON; SCOTT, 1997; WILFORD; BIERWIRTH; CRAIG, 1997; GNOJEK; PRICHYSTAL, 1985), but in this study, they promoted excessive attenuation of values. Th/K only expressed great difference between RO and RL, since this ratio is known to be useful for delineating weathered materials (DAUTH, 1997; WILFORD, 2012). The most contrasting values are in charge of K, followed by eTh, eU and F parameter.

K presented the greatest tracer potential (greater contrasts) not only between rock groups, but also in different weathering degrees (RO *versus* RL). Higher K contents were observed predominantly in PGN, PMF and PPS rock groups, being always higher in RO than RL (Figure 5 A). However, an inverse relationship is observed only for PPP group. This may be related to the greater presence of metamorphic phyllosilicates (mainly muscovite and biotite) present in the shales and phyllites of the PPP group (SUGUIO, 2003), even in highly weathered conditions of RL landscapes. Muscovite can be a stable mineral depending on weathering conditions, and clay minerals are generally formed by the alteration of biotite under certain environmental circumstances (SUGUIO, 2003). The PPP presented mean K values similar to the PGN for RO and RL, mainly due to the composition dominated by clay/mica group of minerals. In contrast, the PPS group, represented by predominantly siliciclastic rocks, has a low K mean values related to the restricted contribution of feldspathic, phyllosilicate and clay mineral components (DICKSON; SCOTT, 1997; WILFORD; BIERWIRTH; CRAIGIG, 1997). Higher mean values were found in PGN rock group probably associated with the occurrence of acidic/intermediate igneous rocks, such as rhyolite, granite, pegmatite, and rocks from the crystalline basement. These rocks have mineralogy with a strong contribution of phyllosilicates, mainly from the mica group, in addition to the significant contribution of potassium feldspar. Rocks from the PMF group also showed a relatively high mean value for K, due to the association with mica-group of minerals such as biotite and phlogopite.

For the radioelements eTh and eU, the highest concentrations were observed in rocks and soils derived from pedogneissic rocks (PGN). The occurrence of these elements is related

to felsic rocks that have higher contents of incompatible elements such as eTh and eU compared to rocks and soils derived from pedomafic materials (PMF) (DICKSON; SCOTT, 1997). For the other groups, PPP and PPS, dominated by metasedimentary and sedimentary rocks, the concentrations of eTh and eU are relatively higher in the rocks of the first group. For sedimentary rocks, the eTh and eU concentrations reflect the source material of the sediments. This makes the correlation difficult since the groups are a set of lithotypes derived from several contributing sources. Except for PPP rock domains, which high contrast between RO and RL is found, eTh values are similar in the different landscapes. For the eU, the higher levels are observed for PGN and PPP, where the contrasts between RO and RL are also higher. Since eTh and eU tend to be typically adsorbed along the weathering, being associated with stable components in the soil, the differences in such values between rock and soil may not be very expressive.

U and Th are typically retained during the weathering of rocks and readily adsorbed to minerals in the clay fraction and iron and aluminum oxides of the soil, tending to concentrate in highly weathered soils (DICKSON; SCOTT, 1997; WILFORD; BIERWIRTH; CRAIG, 1997; TAYLOR; EGGLETON, 2001). Furthermore, the dynamics and redistribution of U and Th in soils tend to be more complex, where different release and adsorption pathways can occur (WILFORD, 2012). Thus, further local analysis of mineral characterization and organic matter content are necessary do better comprehend the biochemistry of such radioelements.

The F parameter (GNOJEK; PRICHYSTAL, 1985; RIBEIRO; MANTOVANI; LOURO, 2015) derives from the potassium contribution and the U/Th ratio. Highly weathered landscape with high K leaching tend to have low values for the F parameter, highlighting the difference in radioelement content between RO and mature landscapes (RL).

In general, it was observed that the advances of weathering and pedogenesis in these landscapes generated different responses in the behavior of radioelements after being released from the primary rocks. This behavior may be due to: a) the nature of the source material; b) dynamics of weathering and pedogenesis of weathered materials; c) geomorphological processes.

3.2 Relationship between gamma-ray data and topographic data

Figure 6 A, B, C, D and E show the elevation profiles (variations of altitude with respect to distance) of each rock grouping under RL (rock outcrops are excluded in this case). Such locations were chosen seeking to contemplate the same horizontal distance (3,000 m), covering

positions from the lower (depositional) to the higher areas. For the same elevation profile, variations of radiometric contents and their rations is displayed, since these topographic variations can influence in the soil mineralogical composition, soil granulometry, and dynamics of soil geochemical elements (RESENDE et al., 2014; RESENDE et al. 2021). This analysis was carried out only for the Red Latosols, since the release dynamics and movement of chemical elements in the rocks is incipient.

It is possible to notice distinctive pattern of radionucleotides accumulation and depletion across topographical variations. Except for PPP group of rocks, higher K and F parameter values are found in depositional areas, with values decreasing towards the higher altitudes, following the K losing → addition model of soil formation reported by Simonson (1959). Latosols, a very deep and polygenetic soil, tend to occur in pretty stable landscape over years, suffering extremely weathering-leaching conditions imposed by climatic conditions (MUGGLER; BUURMAN, 2000). In contrast, U/K and Th/K for PMF, PGN and PPP showed opposite trend (relative lower contents in depositional portions). eTh, U and U/Th contents showed an irregular distribution along the toposequence, showing a smaller influence of the landscape on its geochemical behavior.

The soils derived from PPP presented relatively higher contents for the studied parameters, where it is possible to observe that the Th/K and U/K ratios increased in higher areas. The contents of eU, eTh and U/Th proved to be erratic across the selected landscape. The PPS had the lowest K contents (relatively higher contents in the lower portions). eTh, eU, Th/K, U/K and U/Th showed similar trends: erratic distribution along the toposequence. The F factor, on the other hand, presented values inversely proportional to the elevation, as well as the Red Latosols derived from PMF, contents among the groups of rocks. Moreover, soils derived from PMF and PGN group or rocks presented relatively higher amplitudes of Th/K, U/K, intermediate levels of K and erratic levels of eTh, eU and U/Th. The highest amplitude of Th/K and U/K ratios related to PMF stands out.

Figure 6 - Topographic vertical sections (altitude x distance) and respective K (%), eTh (ppm) and eU (ppm) values, their different relationships and F Parameter in landscapes of Red Latosols in different rock domains

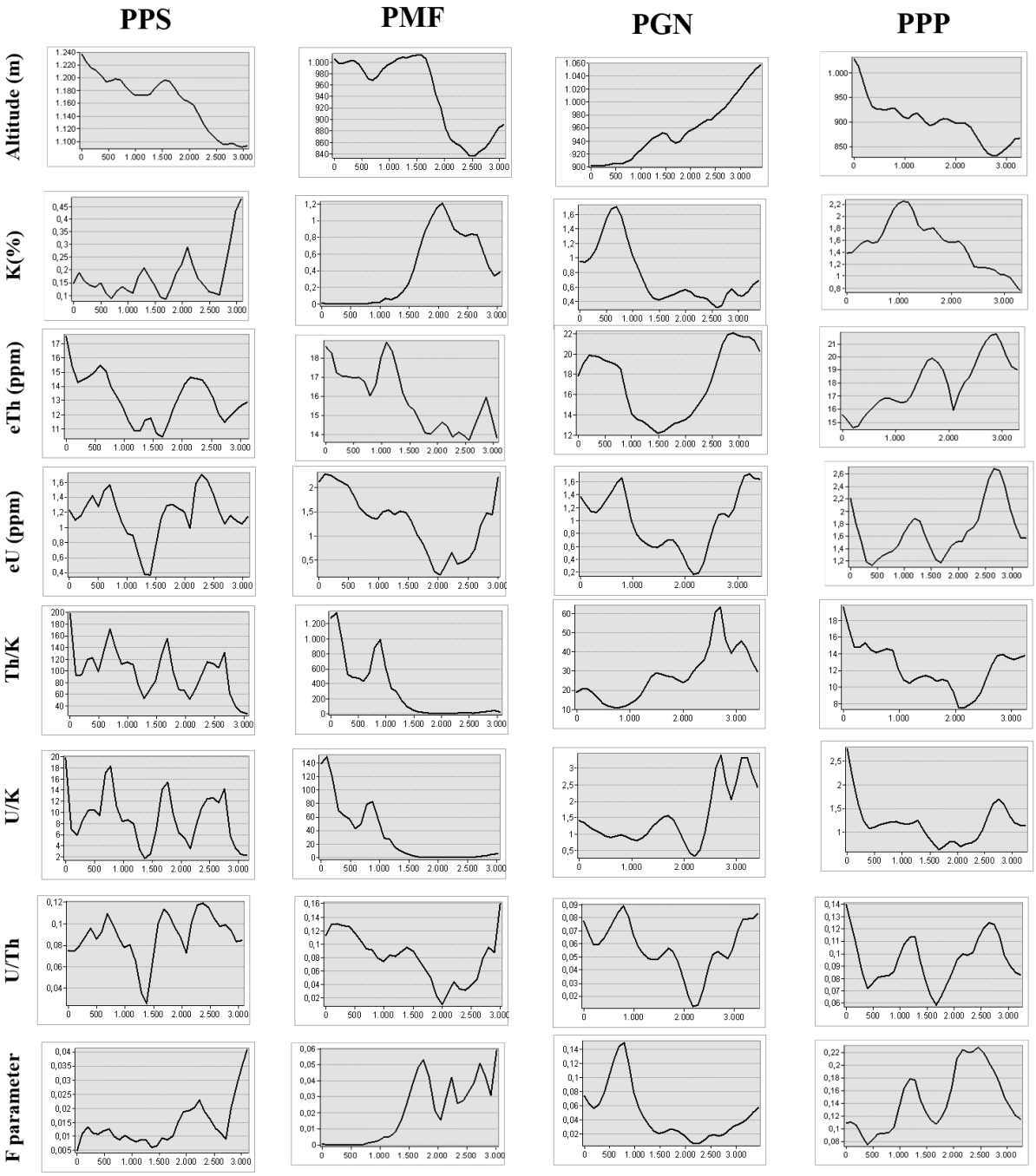

Legend: PPS = Pedopsamitic; PMF = Pedomafic; PGN = Pedogneissic; PPP= Poor Pedopelitics.
Source: Author (2021)

3.3 Principal Component Analysis (PCA)

PCA was performed for RO (Figure 7 A) and RL (Figure 7 B) dataset in order to understand the importance and how relief and climate attributes influence on radioelements in such contrasting landscapes. The first and second axis explains 62% of the data variation for

RO landscapes and 58% for RL landscapes (Figure 7). It is noteworthy that variables importance (size of vectors, the bigger the more important), as well as how environmental data correlates with radionucleotides behaved differently in each PCA, reinforcing the contrasting characteristics of the environments selected.

In the first axis of both PCA, most of climate and paleoclimate information are closed together, revealing higher correlation with each other (multicolinearity), except for the paleoclimate variable mgmidbi12 in the PCA of the RL landscapes (Figure 7 B). These variables stand out in the first axis with positive eigenvectors. The climatic variables showed a relatively strong positive correlation with the DEM and relative slope (Relative_S) terrain variables. However, except for the variable mgmidbi12 in the PCA of the RL landscapes, there was no positive correlation between the climatic variables and the variables extracted from the gamma-ray spectrometry survey (K, Th, U, Th/K, U/K, U/Th, F Parameter).

For the PCA diagrams, the second axis has strong influence of K, F Parameter, Texture, TRI and Slope with positive eigenvectors. On the other hand, Th/K, U/K and TWI present negative eigenvectors in both PCAs. For the RL landscape PCA the second axis also presents a significant influence of the positive eigenvector of the mgmidbi12 variable (Figure 7 B). The climate model represented by the variable mgmidbi12 shows the annual total precipitation of 6,000 years ago. This period presents a higher precipitation rate when compared to the current period and may be related to an interglacial period. Interglacial periods have hot and humid weather which may favor pedogenesis and a deeper soil profile and consequently the genesis of Red Latosols (RESENDE et al. 2019). Paleoclimate is an important characteristic of Latosols genesis, since they are considered polygenetic soils because of the very long periods of soil formation, and the different climates of the past (MUGGLER; BUURMAN, 2000).

The variables U, Th and U/Th do not present a significant influence in the variation of the data, but it is interesting to note the differences in the behavior of these variables between one circle and another. For the RO, U and U/Th landscapes showed a low to medium positive correlation in the second axis of the PCA and so on with the variables that are grouped there; Th showed a low degree of correlation on both axes. For the RL, U and Th landscapes showed a slightly positive correlation with the climatic variables grouped in the first axis; the U/Th ratio showed a weak correlation on both axes.

The strong influence of K and F Parameter as well as the overlapping of their effects and the weak influence of U, Th and U/Th corroborated the results obtained in the boxplots where it was possible to observe that the first two variables showed greater differentiation in the concentration of K between the landscapes. The influence of the Th/K and U/K ratios, due

to the low nature of the values, was more noticeable in the PCA analysis when compared to the boxplot.

The principal component analyzis corroborates the following topics: i) there was an important positive correlation between variables K, F Parameter, Texture, TRI and Slope; ii) the variable mgmidbi12 proved to be important in correlating the behavior of radioelements to RL landscapes; iii) pedogenetic processes influence the redistribution of Th and U in the landscape according to Dickson & Scott (1997); U and Th have a more complex behavior in the weathering and pedogenesis profiles.

Figure 7 - PCA for rock outcrops (A) and Red Latosols landscapes (B).

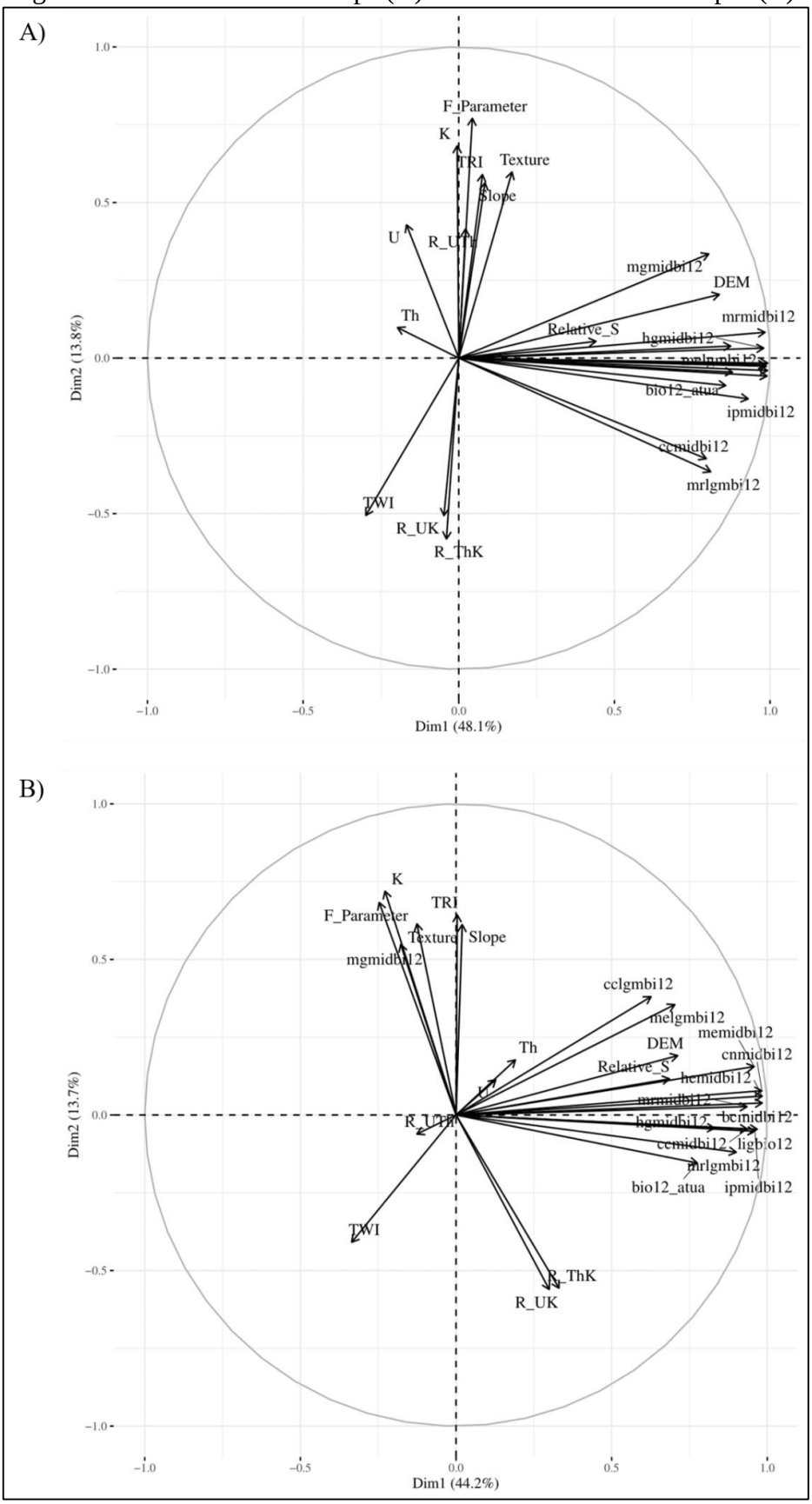

Legend: TWI = topographic wetness index; TRI = Terrain Ruggedness Index; DEM = digital elevation model; Relative_S = Relative Slope.
Source: Author (2021)

4 CONCLUSIONS

I) Gamma spectrometry images must be analyzed in the spatial context, since the relationships between radionucleotides and environment might be complex;

II) The applied methodology was able to show how the advance of weathering and pedogenesis act in soil geochemistry (eK, eTh and eU) on regional scale;

III) Gamma spectrometric images, mainly through the K and F Parameter variables, have an adequate potential in differentiating soil parent materials in tropical environments, especially when associated with topographic parameters as Texture, TRI and Slope;

IV) The potential of gamma spectrometric images in mapping soil parent material can be improved if applied in a well-characterized area in terms of regolith and lithology knowledge. It is recommended to study first a smaller area using geological maps at more detailed scale in order to calibrate geological materials with gamma spectrometric responses.

REFERENCES

BOEHNER, J.; CONRAD, O. Module Relative Heights and Slope Positions. SAGA-GIS Module Library Documentation; 2008.

BOYLE, R. W. Geocheical Prospecting for Thorium and Uranium Deposits. Developments in economic geology, n.16, p. 71-78, 1982.

CODEMGE. **Levantamento Aerogeofísico**. Disponível em: <http://www.codemge.com.br/atuacao/mineracao/levantamento-aerogeofisico/>. Acesso em: 16 maio. 2019.

CODEMIG; CPRM. **Levantamento Aerogeofísico de Minas Gerais área 02: Pitanguí – São João del Rei - Ipatinga**. Relatório final do levantamento e processamento dos dados magnetométricos e gamaespectrométricos, Volume I, 2006. Lasa Engenharia e Prospecções S.A.

CODEMIG; CPRM. **Levantamento Aerogeofísico de Minas Gerais área 07: Patos de Minas - Araxá - Divinópolis**. Relatório final do levantamento e processamento dos dados magnetométricos e gamaespectrométricos, 2006. Lasa Engenharia e Prospecções S.A.

CODEMIG; CPRM. **Levantamento Aerogeofísico de Minas Gerais área 14: Poços de Caldas - Varginha - Andrelândia**. Relatório final do levantamento e processamento dos dados magnetométricos e gamaespectrométricos, 2011. Lasa Engenharia e Prospecções S.A.

CODEMIG; CPRM. **Levantamento Aerogeofísico de Minas Gerais área 15: Juiz de Fora – Cataguases - Manhuaçu**. Relatório final do levantamento e processamento dos dados magnetométricos e gamaespectrométricos, 2011. Lasa Engenharia e Prospecções S.A.

CONRAD, O. Tool Slope, Aspect, Curvature. **SAGA-GIS Tool Library Documentation**, 2001.

CONRAD, O. Module Topographic Wetness Index (TWI). **SAGA-GIS Module Library Documentation**, 2003

CONRAD, O.; BECHTEL, B.; BOCK, M.; DIETRICH, H.; FISCHER, E.; GERLITZ, L.; WEHBERG, J.; WICHMANN, V.; BOHNER, J. System for Automated Geoscientific Analyses (SAGA), v. 2.1.4. **Geosci. Model Dev**., 8, 1991–2007. 10.5194/gmdd-8-2271-2015.

CONRAD, O. Module Terrain Ruggedness Index (TRI). **SAGA-GIS Module Library Documentation**, 2010.

CONRAD, O. Tool Terrain Surface Texture. **SAGA-GIS Tool Library Documentation**, 2012.

COOK, S. E. et al. Use of airborne gamma radiometric data for soil mapping. **Australian Journal of Soil Research**, v. 34, n. 1, p. 183–194, 1996.

CPRM. **Levantamentos Geológicos e Integração Geológica Regional - Atlas Aerogeofísico do Estado de Rondônia.** Porto Velho: 2020.

CPRM. **Geodiversidade do Estado de Minas Gerais**. Belo Horizonte: 2010. Programa Geologia do Brasil.

CPRM. **Mapa geológico do estado de Minas Gerais**. Belo Horizonte: 2003. Escala 1:1.000.000.

CPRM. **Projeto Aerogeofísico São José dos Campos-Resende.** Relatório final do levantamento e processamento dos dados magnetométricos e gamaespectrométricos, 2013.

MELLO, D. C. et al. Applied gamma-ray spectrometry for evaluating tropical soil processes and attributes. **Geoderma**, v. 381, p. 114736, 2021.

DAUTH, C. Airborne magnetic, radiometric and satellite imagery for regolith mapping in the Yilgarn Craton of Western Australia. **Exploration Geophysics** v. 28, p. 199–203, 1997.

DICKSON, B. L.; SCOTT, K. M. Interpretation of aerial gamma-ray surveys-adding the geochemical factors. **AGSO Journal of Australian geology & geophysics**, v. 17, n. 2, p. 17–200, 1997.

FEAM. **Mapa de Solos do estado de Minas Gerais: legenda expandida**. Belo Horizonte: FEAM/UFV/CETEC. 2010. 49p.

FORTIN, R.; HOVGAARD, J.; BATES, M. Airborne Gamma-Ray Spectrometry in 2017: Solid Ground for New Development. **Airborne Geophysics**, p. 129-138, 2017.

GNOJEK, I.; PRICHYSTAL, A. A New Zinc Mineralization Detected by Airborne Gamma-ray Spectrometry in Northern Moravia (Czechoslovakia). **Geoexploration**, v. 23, p. 491–502, 1985.

HARRISS, R. C.; ADAMS, J. A. S. Geochemical and mineralogical studies on the weathering of granitic rocks. **American Journal of Science**, v. 264, n. 2, p. 146–173, 1966.

HUSSON, F.; LE, S.; JÉRÔME, P. Exploratory Multivariate Analysis by Example Using R. 2nd. ed. Chapman and Hall/CRC, 2017.

JENNY, H. **Factores of Soil Formation: A System of Quantitative Pedology**. New York, NY, USA: McGraw-Hill Book Co., 1941.

KENT, M. & COKER, P. **Vegetation description and analysis**. Baffins Lane, John Wiley & Sons, 1992. 363p.

LACOSTE, M.; LEMERCIER, B.; WALTER, C. Regional mapping of soil parent material by machine learning based on point data. **Geomorphology**, v. 133, n. 1–2, p. 90–99, 1 out. 2011.

LEMIÈRE, B. A review of pXRF (field portable X-ray fluorescence) applications for applied geochemistry. **Journal of Geochemical Exploration**, v. 188, p. 350–363, 1 maio 2018.

MACHADO, D. F. T. et al. Soil type spatial prediction from Random Forest: different training datasets, transferability, accuracy and uncertainty assessment. **Scientia Agricola**, v. 76, n. 3, p. 243–254, 2019.

MINTY, B. R. S. Fundamentals of airborne gamma-ray spectrometry. **AGSO Journal of Australian Geology & Geophysics**, v. 17, n. 2, p. 39–50, 1997.

MOONJUN, R. et al. Application of airborne gamma-ray imagery to assist soil survey: A case study from Thailand. **Geoderma**, v. 289, p. 196–212, 1 mar. 2017.

MUGGLER, C. C.; LOPES, L. M.; RESENDE, M. Geologia para estudantes de Ciências Agrárias: a experiência da Universidade Federal de Viçosa. In: Simpósio de Especialização em Ensino de Geociência, 1990, Campinas, SP. **Anais...** Campinas, SP: UNICAMP, 1990. p. 113-118.

MUGGLER, C. C.; BUURMAN, P. Erosion, sedimentation and pedogenesis in a polygenetic oxisol sequence in Minas Gerais, Brazil, **Catena,** v. 41, Issues 1–3, p. 3-17, 2000.

OTTO-BLIESNER, BETTE L. et al. Modeling and Data Syntheses of Past Climates Carbon and Nutrient Cycling in the Southwestern Atlantic Ocean. Eos, **Transactions American Geophysical Union**, v. 90, n. 11, 2009.

PACIULLO, F. V. P. et al. Contribuição à geologia do sul de Minas Gerais edição das folhas 1: 50.000 Itumirim, Itutinga, Madre de Deus, Luminárias, Minduri e Andrelândia. **Anuário do Instituto de Geociências**, v. 19, p. 123–142, 1996.

PEDROSA-SOARES, A. C. et al. **Nota explicativa dos mapas geológico, metalogenético e de ocorrências minerais do Estado de Minas Gerais**. Belo Horizonte.1994.

RESENDE, M. et al. **Propriedades do solo e interpretação**. In: RESENDE, M. et al. Pedologia base para distinção de ambientes. 6º Ed. Editora UFLA, Lavras, MG, p. 378, 2014.

RESENDE, M.; CURI, N.; POGGERE, G. C.; BARBOSA, J. Z.; POZZA, A. A. A.; TEIXEIRA, A. F. S. Pedologia, Fertilidade, Água e Planta: Inter-relações e aplicações. 263. ed. Lavras - MG: Editora UFLA, 2021.

RESENDE, M. **Pedologia**. Viçosa: Universidade Federal de Viçosa, 1982. 100p.

RESENDE, M. et al. **Da Rocha ao Solo: enfoque ambiental**. 1. ed. Lavras: UFLA, 2019.

RIBEIRO, A. et al. Síntese geológica regional do Bloco Ocidental, Campos das Vertentes e Sul de Minas. **Geologia e Recursos Minerais do Sudeste Mineiro. Projeto Sul de Minas Etapa I**. p.51-152, 2003.

RIBEIRO, V. B.; MANTOVANI, M.; LOURO, V. H. A. Aerogamaespectrometria e suas aplicações no mapeamento geológico. Terrae Didatica, v. 10, n. 1, p. 29, 2015.

SÁ JÚNIOR, A. **Aplicação da classificação de Köppen para o zoneamento climático do estado de Minas Gerais**. 2009. Dissertação, Mestrado - Universidade Federal de Lavras, Lavras, 2009.

SCHAETZL, R. J.; ANDERSON, S. **Soils: genesis and geomorphology**. New York: Cambridge University Press, 2005.

SIMONSON, R.W. Outline of a generalized theory of soil genesis. **Soil Science Society of America Proceedings** v. 23, 152–156, 1959.

SILVA, S. H. G. et al. Proximal Sensing and Digital Terrain Models Applied to Digital Soil Mapping and Modeling of Brazilian Latosols (Oxisols). **Remote Sensing**, v. 8, n. 614, 2016.

SUGUIO, K. **Geologia Sedimentar**. São Paulo: editora Edgard Blücher Ltda, 2003. 400p.

TAYLOR, M. J. et al. Relationships Between Soil Properties and High-Resolution Radiometrics, Central Eastern Wheatbelt, Western Australia. **Exploration Geophysics**, v. 33, n. 2, p. 95–102, 6 jun. 2002.

TAYLOR, G.; EGGLETON, R. A. **Regolith geology and geomorphology**. J. Wiley, 2001.

TAYLOR, K. E.; STOUFFER, R. J.; MEEHL, G. A. An overview of CMIP5 and the experiment design. **Bulletin of the American Meteorological Society**, v. 93, n. 4, p. 485–498, 2012.

THIESSEN, K. et al. Modelling radionuclide distribution and transport in the environment. **Environmental Pollution**, v. 100, n. 1–3, p. 151–177, 1 jan. 1999.

XU, T.; HUTCHINSON, M. F. New developments and applications in the ANUCLIM spatial climatic and bioclimatic modelling package. **Environmental Modelling and Software**, v. 40, p. 267–279, 2013.

WILFORD, J. R.; BIERWIRTH, P. N.; CRAIG, M. A. Application of airborne gamma-ray spectrometry in soil/regolith mapping and applied geomorphology. **AGSO Journal of Australian Geology and Geophysics**, v. 28, n. 16, p. 201–216, 1997.

WILFORD, J.; MINTY, B. The use of airborne gamma-ray imagery for mapping soils and understanding landscape processes. **Developments in Soil Science**, v. 31, p. 207-218, 2007.

WILFORD, J. A weathering intensity index for the Australian continent using airborne gamma-ray spectrometry and digital terrain analysis. **Geoderma**, v. 183–184, p. 124–142, 1 ago. 2012.